Article

Not peer-reviewed version

# Design, Synthesis, and Evaluation of Antinociceptive Properties of Novel CBD-Based Terpene-Cinnamoyl-Acyl-Hydrazone Analogues

Mikaela Lucinda de Souza , João Pedro Barros de Paiva , Graziella dos Reis Rosa Franco , Vanessa Silva Gontijo[1] , Marina Amaral Alves[2] , Hygor Marcos Ribeiro de Souza , Anna Carolina Pereira Lontra , Eduardo Araújo de Oliveira , Thaís Biondino Sardella Giorno , Isabella Alvim Guedes , Laurent Emmanuel Dardenne , Patrícia Dias Fernandes * , Claudio Viegas Jr. *

Posted Date: 24 April 2025

doi: 10.20944/preprints202504.2053.v1

Keywords: CBD analogues; antinociceptive activity; cannabidiol-based analogues; acute pain; bioactive acyl-hydrazone derivatives

 doi:10.20944/preprints202504.2053.v1



*Article*

# Design, Synthesis, and Evaluation of Antinociceptive Properties of Novel CBD-Based Terpene-Cinnamoyl-Acyl-Hydrazone Analogues

**Mikaela Lucinda de Souza [1,†], João Pedro Barros de Paiva [2,†], Graziella dos Reis Rosa Franco [1], Vanessa Silva Gontijo [1], Marina Amaral Alves [3], Hygor Marcos Ribeiro de Souza [3], Anna Carolina Pereira Lontra [2], Eduardo Araújo de Oliveira [2], Thaís Biondino Sardella Giorno [2], Isabella Alvim Guedes [4], Laurent Emmanuel Dardenne [4], Patrícia Dias Fernandes [2,*] and Claudio Viegas Jr.[1,*]**

[1] Federal University of Alfenas, Institute of Chemistry, PeQuiM- Laboratory of Research in Medicinal Chemistry, Alfenas-MG, 37133-840, Brazil

[2] Federal University of Rio de Janeiro, Institute of Biomedical Sciences, Laboratory of Pharmacology of Pain and Inflammation, Rio de Janeiro-RJ, 21941-577, Brazil

[3] Federal University of Rio de Janeiro, Institute of Chemistry, Laboratory of Metabolomics – LabMeta/LADETEC, Rio de Janeiro – RJ, 21941-598, Brazil

[4] National Laboratory for Scientific Computing, Molecular Modeling in Biological Systems Group, Petrópolis-RJ, 25651-075, Brazil

* Correspondence: patricia.dias@icb.ufrj.br, +55 (21) 3938-6480 (P.D.F); claudio.viegas@unifal-mg.edu.br, +55 (35) 3701-1881 (C.V.J.)

† These authors contributed equally to this work.

**Abstract: Background/Objectives**: Cannabidiol (CBD) has been reported for its antinociceptive, anti-inflammatory, and neuroprotective activities. However, several legal restrictions for its medicinal uses, and even research, have contributed to the development of synthetic analogues. Therefore, the aim of this study was the design and synthesis of a novel series of CBD-based structural analogues, and the *in vivo* evaluation of their potential antinociceptive activity. **Methods**: Using a two-step synthetic route, 26 new terpene-cinnamoyl acyl-hydrazone analogues were obtained and were submitted *in vivo* screening in the classical formalin-induced paw edema and hot plate assays. **Results**: Compounds PQM-292, PQM-293, PQM-295, PQM-307, PQM-308, and PQM-309 exhibited the best results in the neurogenic phase (1st Phase) of the formalin-induced licking response, showing comparable results to morphine. Notably, in the inflammatory phase (2nd Phase), compound PQM-292 exhibited the best anti-inflammatory activity. Interestingly, in the hot plate model, other six compounds (PQM-274, PQM-291, PQM-294, PQM-304, PQM-305, and PQM-378) showed the best antinociceptive activity in comparison to morphine, especially PQM-274 which exhibited an antinociceptive effect almost equivalent to the reference drug. Interestingly, these findings suggested that these bioactive compounds, despite their structural similarity, act through different mechanisms, which were investigated by molecular docking with CB1, CB2, and TRPV1 receptors. *In silico* results indicated that the most active compounds should act through different mechanisms, probably involving interactions with TRPA1. **Conclusions**: Therefore, due to the promising antinociceptive activity observed for these highlighted compounds, particularly for PQM-292 and PQM-274, without apparent toxicity and psychoactive effects, and the possible involvement of diverse mechanisms of action, these compounds could be considered as promising starting points to the development of new drug candidate prototypes of clinical interest.

**Keywords:** CBD analogues; antinociceptive activity; cannabidiol-based analogues; acute pain; bioactive acyl-hydrazone derivatives

 doi:10.20944/preprints202504.2053.v1



## 1. Introduction

*Cannabis* species have been used since ancient times by humans for health purposes. Among the 538 active secondary metabolites identified in *Cannabis*, more than 120 cannabinoids have been identified (ca. 22%) [1,2]. Cannabidiol ((-)-CBD, 1, Figure 1) is a non-psychoactive cannabinoid, which was first isolated from *C. sativa* in 1940. Despite its apparent pharmacological promiscuity, evidenced by its wide range of biological properties and potential interaction with multiple molecular targets, CBD is currently considered a clinically safe drug, with few and relatively smooth adverse effects, including diarrhea, appetite changes, among others. The safety doses are dependent on the route of administration, and when administrated orally the well-tolerated doses are up to 1600 mg [3]. The chemical structure of CBD is constituted by a monoterpene system linked to a 2-6-di-hydroxylated-4-*n*-pentyl-aryl ring and is naturally available only in the *trans*-relative configuration. The bioactivity of CBD seems to be, at least in part, related to the presence of the two hydroxyl groups at the aromatic ring (Figure 1, in blue), as well as the methyl group on the terpene subunit (Figure 1, in green), given that these groups can interact by different modes with amino acid residues in different molecular targets. In addition to the hydroxyl groups, the *n*-pentyl side chain appears to be essential for the antioxidant properties and could contribute to lipophilicity [1]. Amidst the cannabinoids, it was noted that aryl-substituted meroterpenoids (a special class of natural products derived from mixed terpenoid biogenesis) [4], such as CBD, have shown diverse pharmacological properties, such as anti-inflammatory, immunomodulatory [5], antioxidant, neuroprotective, an antimicrobial, and analgesic, among others [1].

To date, over 65 molecular targets have been reported to interact with CBD, such as transient receptor potential ankyrin 1 (TRPA1), transient receptor potential cation channel family (TRP), cannabinoid receptors type 1 (CB1) and type 2 (CB2), which are the main constituents of the endocannabinoid system (ECS) [3]. Such wealth of related targets favors different biological activities and pharmacological effects, as the above mentioned [3,6,7]. Regarding the TRP channels, they are located in the plasma membrane of animal's cells, and are related to the analgesic properties of CBD, especially TRPV1. CBD was observed to effectively act against neuropathic pain, a chronic painful condition that impacts 20-25% of individuals worldwide. In addition, CBD can modulate the uptake of neurotransmitters such as dopamine, noradrenaline, GABA, and serotonin, which reinforce its antinociceptive properties [2].

Regarding the anti-inflammatory effects of CBD, it was discovered that it plays a role in the reduction of levels of pro-inflammatory markers, such as interleukin (IL) IL-1β [1] and IL-6 and, in turn, contributing to counteract chronic pain condition [2]. Moreover, CBD interacts direct and indirectly with the ECS, showing lower affinity for CB1, mainly expressed on the brain, than for CB2 receptors, which are most abundant in immune cells. Other pathways of action attributed to CBD involve interactions with the G protein-coupled receptors (GPCRs) and inhibition of arachidonic acid metabolites [2,8]. All these findings corroborate with the difficulties underlying the comprehension of CBD's pharmacokinetics, reinforcing the need to more detailed studies about all potential molecular targets, and possible modifications on the structure of CBD which could result in an enhanced pharmacological profile.

As the natural cannabinoids, their synthetic derivatives have shown interesting biological activities [9], as exemplified by compounds HU-443 (**2**, Figure 1) and HU-308 (**3**), which exhibit significant anti-inflammatory and analgesic activities, acting as selective CB2 ligands, and the anti-inflammatory derivative DMH-CBD (**4**, Figure 1) [10]. It is important to note that the poor bioavailability of CBD is a major problem in evaluating its therapeutical effectiveness [1], stimulating the search for novel structurally CBD-based analogues. Literature data show that most usual modifications proposed by authors were related to the *n*-pentyl side-chain, in the hydroxy-substituents in the aromatic ring, or in the methyl groups in the terpene subunit. Structural changes in (-)-CBD also included stereochemical aspects, including the synthesis of its enantiomer (+)-CBD (**5**, Figure 1), which showed a better affinity for cannabinoid receptors, with a slight affinity for CB1. Hydrogenation of (-)-CBD at the isopropenyl functionality led to H2-CBD (**6**, Figure 1), which

 doi:10.20944/preprints202504.2053.v1



exhibited significant anti-inflammatory activity against ROS, nitric oxide and tumor necrosis factor alfa (TNF-$\alpha$), and higher affinity for CB1 [11]. Literature shows that alkylamides can bind to the CB2 receptor, with a stronger interaction than the endogenous cannabinoids [12].

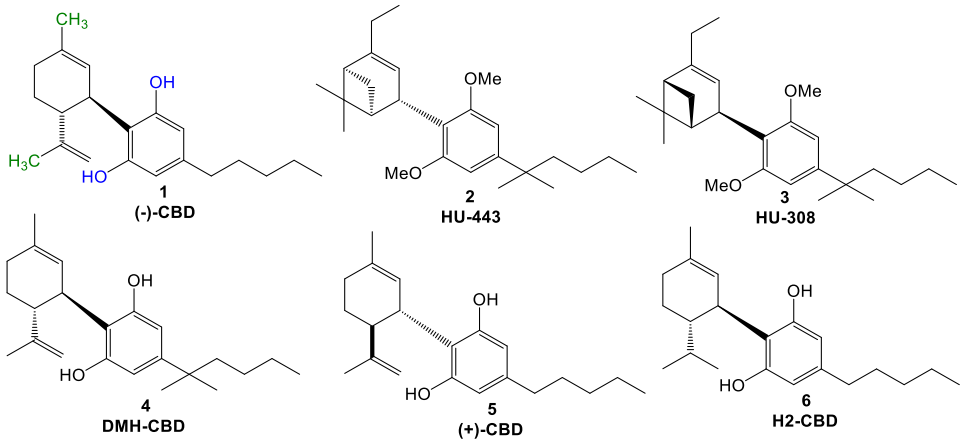


**Figure 1.** Chemical Structures of (-)-CBD (**1**), HU-443 (**2**), HU-308 (**3**), DMH-CBD (**4**), (+)-CBD (**5**), and H2-CBD (**6**).

However, due to intolerance after the addiction to opium, most of the governments prohibit the use of products derived from Cannabis, including CBD [13], which affect research and scientific advances [10]. The legislation about cannabinoids remained outdated, since it dates from 1906, and only in the last decade it was fully revised for medicinal and research uses in many countries. In the USA Cannabis is categorized as marijuana (or "marihuana"), in reference to the fully plant *C. sativa*, encompassing its seeds, leaf, flowers, constituents, and derivatives; and hemp, which refers to the fully plant *C. sativa* when it has a 0.3% concentration of $\Delta^9$-tetrahydrocannabinol ($\Delta^9$-THC), its main psychoactive constituent. In 1937, the USA Congress created the Marihuana Tax Act (Tax Act), regulating and taxing all cannabis analogues, which highly impacted scientific and clinical research, and in 1961, the United Nations Single Convention on Narcotic Drugs determined CBD as an 'liable to abuse' substance [13]. It was only in 2018, with the '2018 Farm Bill' that the USA Congress accepted the classification of hemp with 0.3% of $\Delta^9$-THC and, therefore, CBD derived from a hemp became not classified as a controlled substance, leading to the approving of Epidiolex® by the Food & Drug Administration (FDA), the first CBD-based drug for the treatment of epilepsy and convulsion [9]. Finally, in 2020, following recommendations of the World Health Organization (WHO), the USA removed cannabis from the most restrictive schedule, but it's medicinal use remains illegal in many American regions, and in other countries worldwide [13].

Therefore, given the controversial current global legislation about Cannabis versus the promising therapeutical benefits of CBD and its analogues, many research groups have dedicated efforts to the discovery of new synthetic cannabinoids and CBD-based analogues as drug candidates. Here in, we report for the first time the synthesis and evaluation of a series of terpene-cinnamoyl-acyl-hydrazones, designed as CBD-based structural analogues with potential antinociceptive and anti-inflammatory activity.

## 2. Results

The series of new series of terpene-cinnamoyl-acyl-hydrazones **10a-m**/**11a-m** was designed from the molecular architecture of CBD (**1,** Figure 2), with the carvone structure representing the monoterpene moiety linked to a functionalized aromatic subunit by the introduction of an *N*-acyl-hydrazone spacer. The rationale for the introduction of an *N*-acyl-hydrazone function was based on its potential contribution to the modulation of physical-chemical properties, such as solubility, acidity, and the ability to perform polar interactions, with crucial impact in pharmacokinetics [14–

 doi:10.20944/preprints202504.2053.v1



16]. In addition, *N*-acyl-hydrazone is considered a privileged structure in drug discovery, acting as an important biophore in ligands with anti-inflammatory and antinociceptive activity [17–20]. These structural changes aimed to preserve a similar structural pattern to CBD (**1**), but allowing to study how the structural changes proposed could impact in the pharmacological activity, regarding the position of the endocyclic double bond, changes in the stereochemistry of the *iso*-propenyl group, diverse functionalization on the aromatic ring, removing the alkyl side-chain, and introduction of the *N*-acyl-hydrazone subunit.

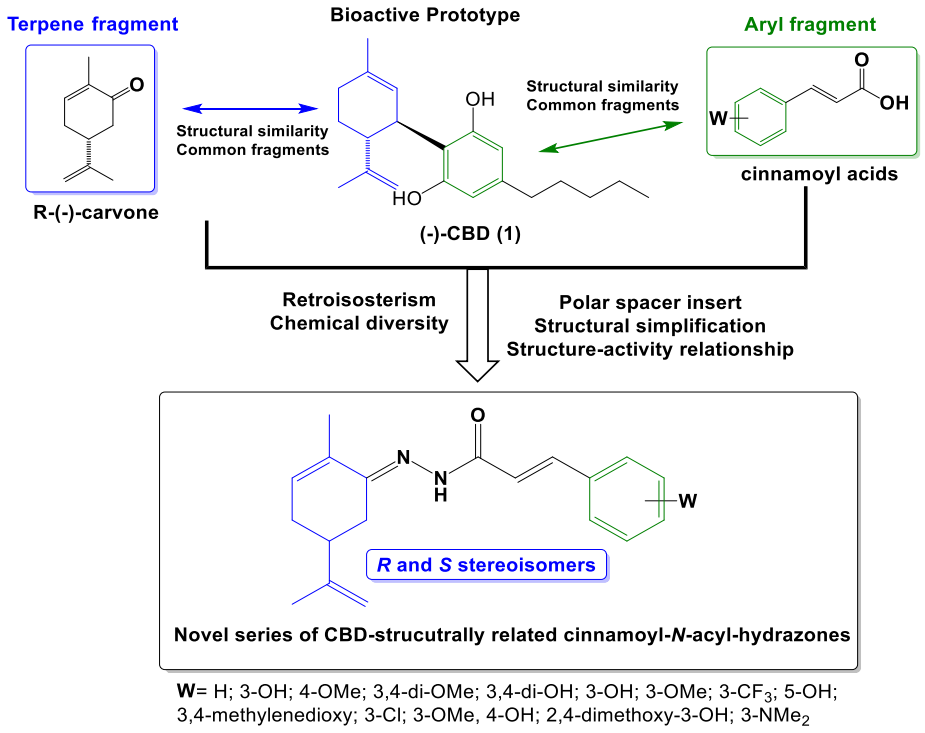


**Figure 2.** Rational structural design of a new series of the CBD-based terpene-cinnamoyl-*N*-acyl-hydrazone analogues.

The synthesis of the target-compounds was performed in a linear two-step route (Figure 3). In a first step, a series of commercially available functionalized cinnamic acids (**7a-m**) was converted into the correspondent hydrazides (**8a-m**) by a hydrazinolysis reaction with hydrazine hydrate, catalyzed by EDAC/HOBt [21]. Next, hydrazides **8a-m** were acid catalyzed reacted with *R*- or *S*-carvone, leading to the desired series of *R*-(**10a-m**) and *S*-*N*-acyl-hydrazones (**11a-m**), respectively. As a result, 26 compounds were obtained as pure solids in 17-83% yields (analytical and spectroscopic data available in the Suppl. Mat.).

 doi:10.20944/preprints202504.2053.v1



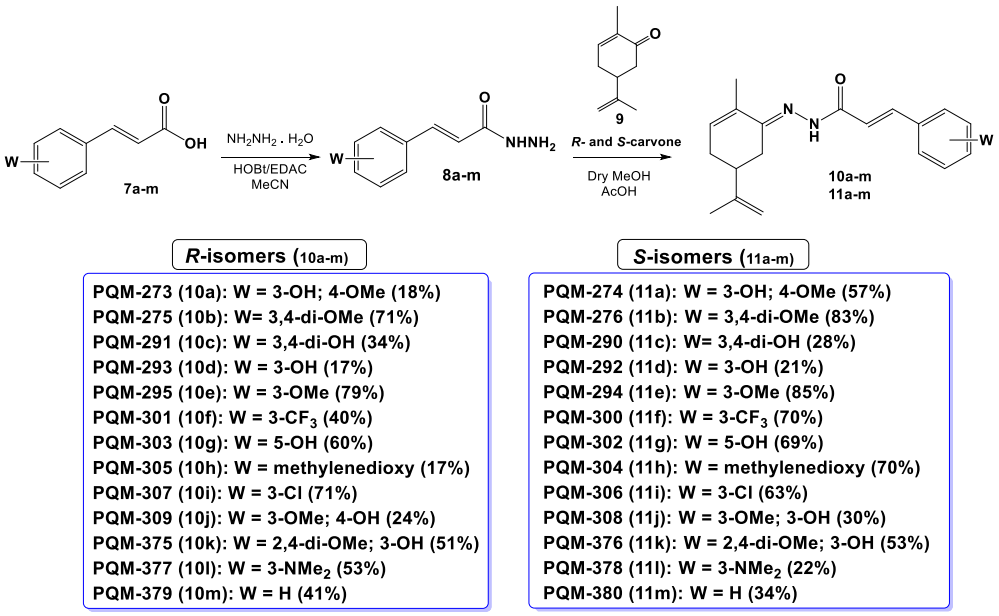


**Figure 3.** Synthetic details for the series of terpene-cinnamoyl-*N*-acyl-hydrazone compounds **10a-m** and **11a-m**.

*2.1. Biological Evaluation*

The first step of biological evaluation was focused on the *in vivo* toxicity of orally administered compounds. After oral administration of a dose of 10 μmol/kg, the animals were observed for possible behavioral changes for a period of 24 hours. Next, blood samples were obtained for hemogram analysis. It was observed that none of the compounds caused behavioral changes (*e.g.*, irritation, drowsiness, convulsions, raised fur, sedation, constipation and diarrhea) or changes in the amounts of water and food intake. In addition, the evaluation of hematological parameters did not indicate any alteration in total and differential cell counts or in hemoglobin, hematocrit, and platelet numbers (data not shown).

Figure 4 demonstrate that pre-treatment of mice with a single dose of 10 μmol/kg of each compound resulted in a significant reduction in the licking behavior in the neurogenic (1st phase) of formalin assay. Except for PQM-375 (**10k**) to PQM-378 (**11l**), and PQM-380 (**11m**), all other compounds caused a reduction in the mice response, particularly for PQM-292 (**11d**), PQM-293 (**10d**), PQM-295 (**10e**), PQM-307 (**10i**), PQM-308 (**11j**), and PQM-309 (**10j**) that exhibited antinociceptive activity comparable to morphine used as reference drug. Regarding the inflammatory phase (2nd phase) of the model, it was observed that PQM-290 (**11c**), PQM-291 (**10c**), PQM-294 (**11e**), PQM-308 (**11j**), PQM-376 (**11k**) and PQM-378 (**11l**) did not show significant ability to reduce formalin-induced inflammatory response. In contrast, PQM-292 (**11d**) stood out among all other compounds for exhibiting the highest antinociceptive effect, almost completely abolishing the response to painful stimuli at a dose of 10 μmol/Kg, even when compared to the positive control groups of morphine and ASA.

The main differences between the two response phases in the formalin-induced paw licking model lie in the fact that the first neurogenic phase, is mainly associated to direct activation of nociceptors and whose painful stimuli is transmitted to the central nervous system (CNS) by afferent C and Aδ-fibers. On the other hand, the second phase, also called as inflammatory phase, the nociceptive effects result from the synthesis and release of inflammatory mediators at the site of formalin injection [22–24]. Thus, the experimental data observed for series 10a-m/11a-m can lead us to infer that some of the compounds may be acting, in some way, reducing or inhibiting the neurogenic response. It could occur due to the inhibition of nociceptors or other receptors responsible for the nociceptive response such as opioid, substance P, kinins receptors. We can also suggest that some of the compounds can present anti-inflammatory effects since they significantly reduced the

 doi:10.20944/preprints202504.2053.v1



second phase of the model, particularly PQM-292 (**11d**). This effect could occur through reduction or inhibition in the formation and/or liberation of a diversity of inflammatory mediators (*i.e.*, prostaglandins and leukotrienes or other inflammatory mediators, such as bradykinin, histamine, and serotonin, as well as cytokine, kinins, glutamate and nitric oxide) [24,25].

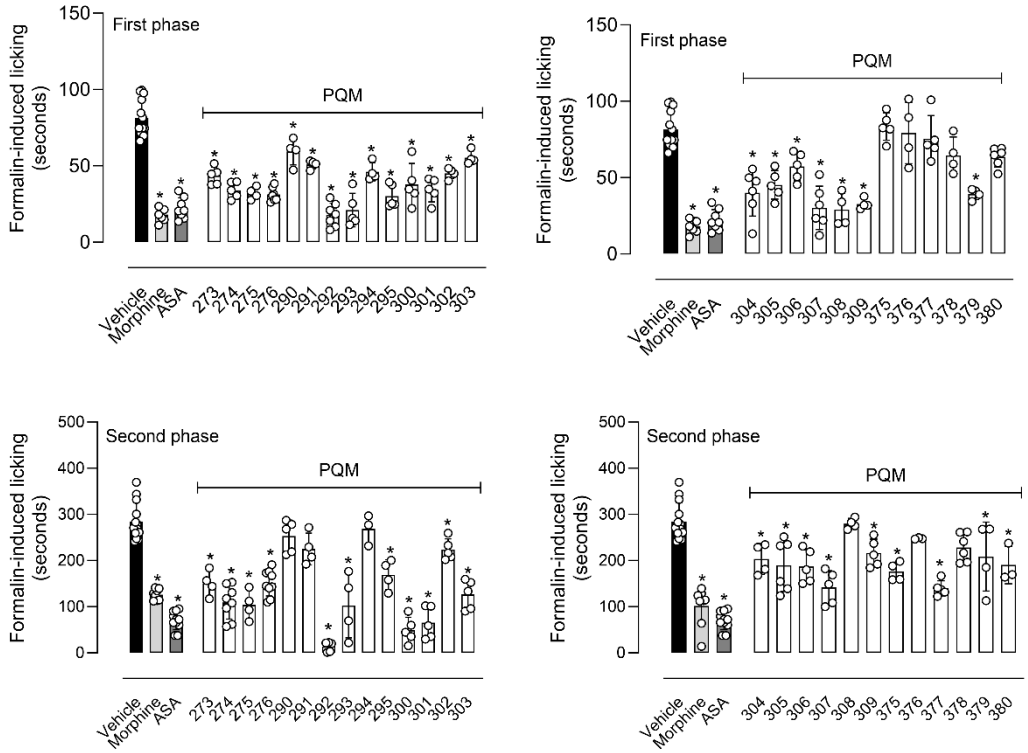


**Figure 4.** Antinociceptive effect of compounds on the licking response induced by formalin in mice. Animals were pretreated with different doses of vehicle, morphine (5 μmol/kg), acetylsalicylic acid (ASA, 1,100 μmol/kg), or compounds (10 μmol/kg), 60 min before the injection of formalin (2.5%/paw). The results are presented as mean ± SD. (n= 5 per group) of the time that the animal spent licking the capsaicin-injected paw. Statistical significance was calculated by ANOVA followed by Tukey´s test. * $p < 0.05$ when compared to vehicle-treated mice.

In a next step, we evaluated the antinociceptive activity of compounds against thermal-induced nociception in the hot plate model. In this assay, the animal is positioned in a warmed plate (55ºC), and the temperature activates nociceptors located in mice paw, transmitting acute nociceptive information to specific regions of the Central Nervous System and, in turn, producing an organized response that result in an elevation of motor response and/or paw licking [26]. As a result, only PQM-295 (**10e**) and PQM-301 (**10f**) did not show a central antinociceptive effect, as depicted by the increased area under the curve (AUC) in Figure 5. Conversely, compounds PQM-274 (**11a**), PQM-291 (**10c**), PQM-294 (**11e**), PQM-304 (**11h**), PQM-305 (**10h**), and PQM-378 (**11l**) exhibited potent antinociceptive effects similarly to that observed for the control group of morphine.

 doi:10.20944/preprints202504.2053.v1



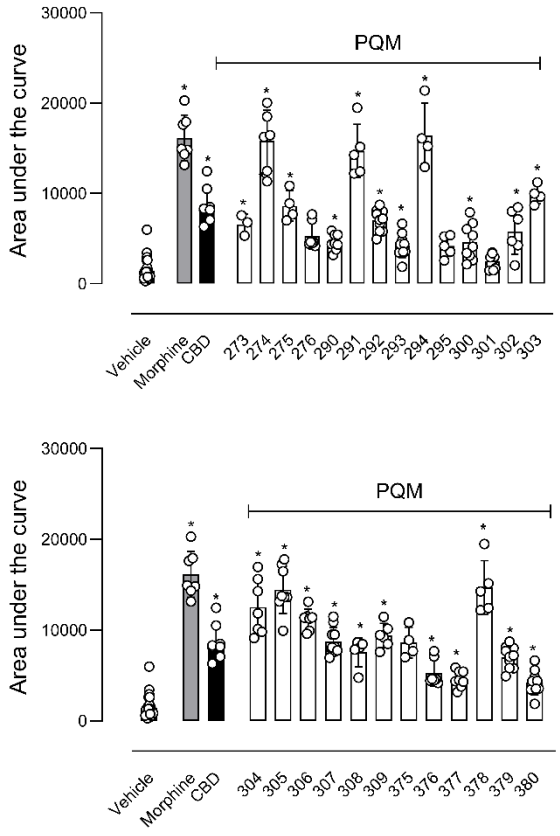


**Figure 5.** Effects of compounds in the thermal-induced nociception (hot plate model). Animals were orally pretreated with morphine (9 μmol/kg), compounds (10 μmol/kg) or vehicle. The results are presented as mean ± SD. (n= 7-10 per group) of area under the curve calculated by GraphPad Prism Software 10.1.2. Statistical significance was calculated by ANOVA followed by Tukey's test. * $p < 0.05$ when comparing to vehicle-treated group.

*2.2. Molecular Docking*

To contribute to a better understanding of possible interactions with cannabinoid receptors potentially involved in the observed antinociceptive properties of the abovementioned compounds, we performed a molecular docking study with compounds **10a-m/11a-m** towards CB1, CB2, and TRPV1 receptors (Table 1). As depicted in Table 1, compounds PQM-275 ($\Delta G_{pred}$= -11.45 kcal/mol, Figure 6A), and PQM-375 ($\Delta G_{pred}$= -11.24 kcal/mol, Figure 6B) were predicted to have the best interaction energy and a slight selectivity for the CB1 receptor, yielding results slightly better than those obtained for CBD ($\Delta G_{pred}$= -10.72 kcal/mol, Table 1). However, none of the compounds were found to make significant interactions with relevant amino acid residues of the protein structure, which was also observed for CBD (**C**, Figure 6), as expected, given its known low affinity for CB1 [3].

**Table 1.** Molecular docking results for binding affinity of the series 10a-m and 11a-m for CB1, CB2, and TRPV1 receptors, with their respective PDB code.

| Compounds | Predicted binding affinity (kcal/mol) | | |
|---|---|---|---|
| | CB1 (8GHV) | CB2 (8GUR) | TRPV1 (8GFA) |
| **PQM-273 (10a)** | -10.75 | -10.71 | -9.25 |
| **PQM-274 (11a)** | -10.72 | -10.77 | -9.74 |
| **PQM-275 (10b)** | -11.45 | -11.04 | -9.61 |
| **PQM-276 (11b)** | -11.21 | -11.12 | -9.71 |
| **PQM-290 (11c)** | -10.58 | -10.37 | -9.09 |

 doi:10.20944/preprints202504.2053.v1



| | | | |
|---|---|---|---|
| **PQM-291 (10c)** | -10.40 | -10.41 | -9.38 |
| **PQM-292 (11d)** | -10.51 | -10.37 | -9.17 |
| **PQM-293 (10d)** | -10.36 | -10.40 | -9.41 |
| **PQM-294 (11e)** | -10.91 | -10.88 | -9.35 |
| **PQM-295 (10e)** | -11.00 | -10.89 | -9.69 |
| **PQM-300 (11f)** | -10.93 | -11.02 | -9.56 |
| **PQM-301 (10f)** | -10.78 | -10.88 | -9.63 |
| **PQM-302 (11g)** | -10.49 | -10.35 | -9.25 |
| **PQM-303 (10g)** | -10.63 | -10.33 | -9.37 |
| **PQM-304 (11h)** | -11.02 | -10.82 | -9.34 |
| **PQM-305 (10h)** | -10.81 | -10.83 | -9.32 |
| **PQM-306 (11i)** | -10.74 | -10.62 | -9.31 |
| **PQM-307 (10i)** | -10.90 | -10.58 | -9.36 |
| **PQM-308 (11j)** | -10.88 | -10.75 | -9.65 |
| **PQM-309 (10j)** | -10.82 | -10.73 | -9.58 |
| **PQM-375 (10k)** | -11.24 | -11.12 | -9.76 |
| **PQM-376 (11k)** | -11.15 | -11.10 | -9.90 |
| **PQM-377 (10l)** | -11.08 | -10.77 | -9.41 |
| **PQM-378 (11l)** | -10.89 | -10.82 | -9.41 |
| **PQM-379(10m)** | -10.56 | -10.36 | -9.33 |
| **PQM-380 (11m)** | -10.52 | -10.32 | -8.92 |
| **CBD** | -10.72 | -10.71 | -8.98 |

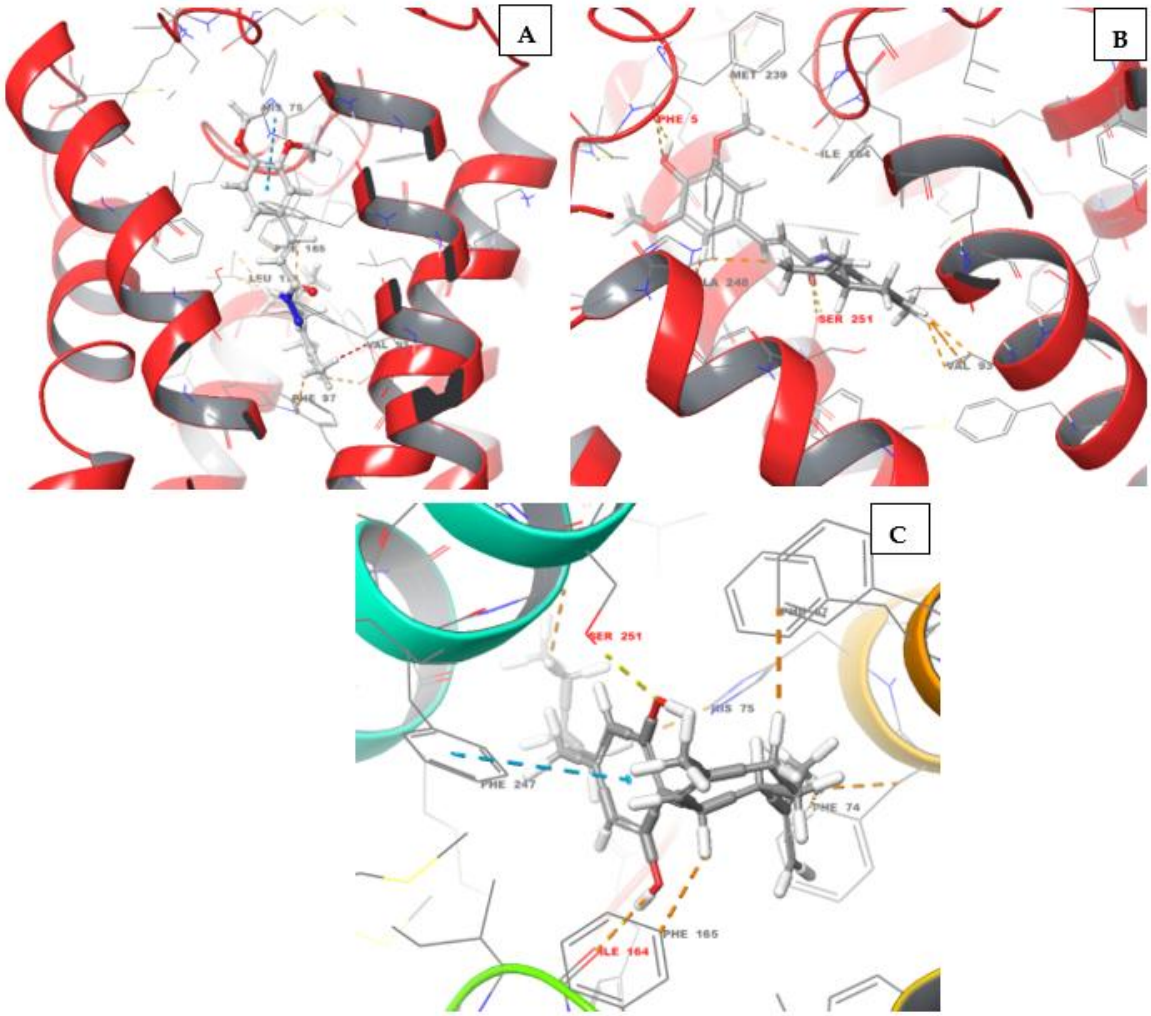

 doi:10.20944/preprints202504.2053.v1



**Figure 6.** Docking results for CB1. **A**: Interactions of PQM-275 with residues of HIS-75, PHE-97, PHE-165, VAL-93, and LEU-173; **B**: Interactions of PQM-375 with residues of VAL-93, MET-239, ILE-164, ALA-248, SER-251 (H-bond interaction), and PHE-5 (H-bond interaction); and **C**: Interactions of CBD with residues of PHE-67, PHE-74, PHE-165, PHE-247, SER-251 (H-bond interaction), ILE-164, and HIS-75. Structural residues according to Liu et al.[27]: $F170^{2.57}$, $174^{2.61}$, $F177^{2.64}$, and $H178^{2.65}$. Residues $F200^{3.36}$ and $W356^{6.48}$ also seems to play a role in the activity.

Interestingly, the analysis of a possible structure-interaction relationship revealed that most compounds substituted with one or two methoxy groups in the aromatic ring, regardless the stereochemistry at the terpene subunit, such as PQM-275, PQM-276, PQM-375, PQM-376, PQM-294, PQM-295, PQM-300, PQM-307, PQM-308, and PQM-309, as well as the two 3-dimethylamine analogues PQM-377, PQM-378, the 5-hydroxy analogue PQM-303, and PQM-379 tend to adopt similar orientation and establish similar interactions, with the terpene subunit facing the interior of the protein cavity, as highlighted for PQM-375 in Figure 7A. In contrast, the 3,4-methylene-dioxy analogue PQM-304, assumed a different orientation, allowing interactions with the terpene subunit facing the exterior of the cavity (Figure 7B). On the other hand, compounds, PQM-273, PQM-274, PQM-290, PQM-291, PQM-380, PQM-292, PQM-293, PQM-301, PQM-302, PQM-305, PQM-306, and were predicted to assume completely different conformation with the terpene subunit twisted to the opposite side of those previously mentioned, as highlighted for PQM-292 in Figure 7C.

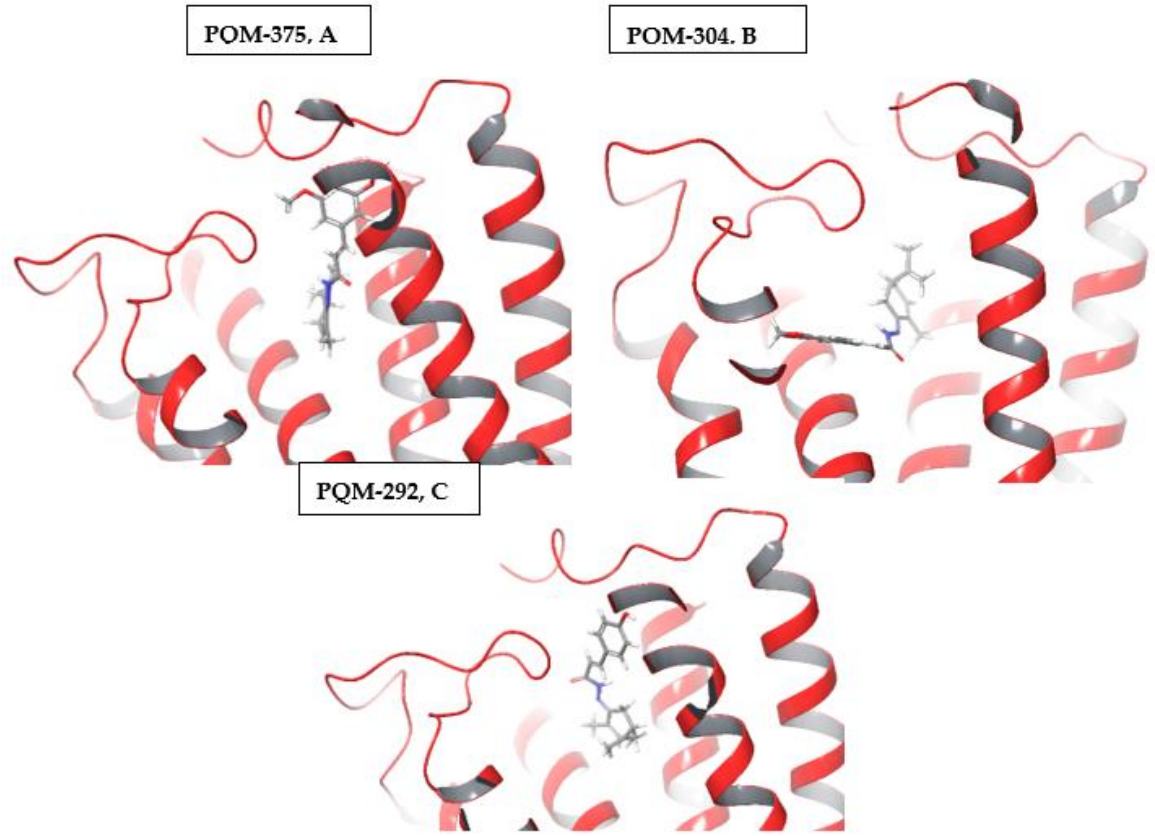


**Figure 7.** Distinct positions that compounds were predicted in the docking results for CB1.

Regarding CB2 receptor, we identified that only in compounds PQM-273, PQM-275, PQM-301, and PQM-307 the terpene subunit was facing the interior of the protein cavity. Furthermore, although few significant interactions predicted, we observed that the hydroxylated compounds PQM-290 (3,4-di-OH), PQM-302 (5-OH), and PQM-303 (5-OH), as well as the 3-methoxylated analogue PQM-295, were predicted to perform a H-bond interaction with the THR93 residue (Figure 8).

 doi:10.20944/preprints202504.2053.v1



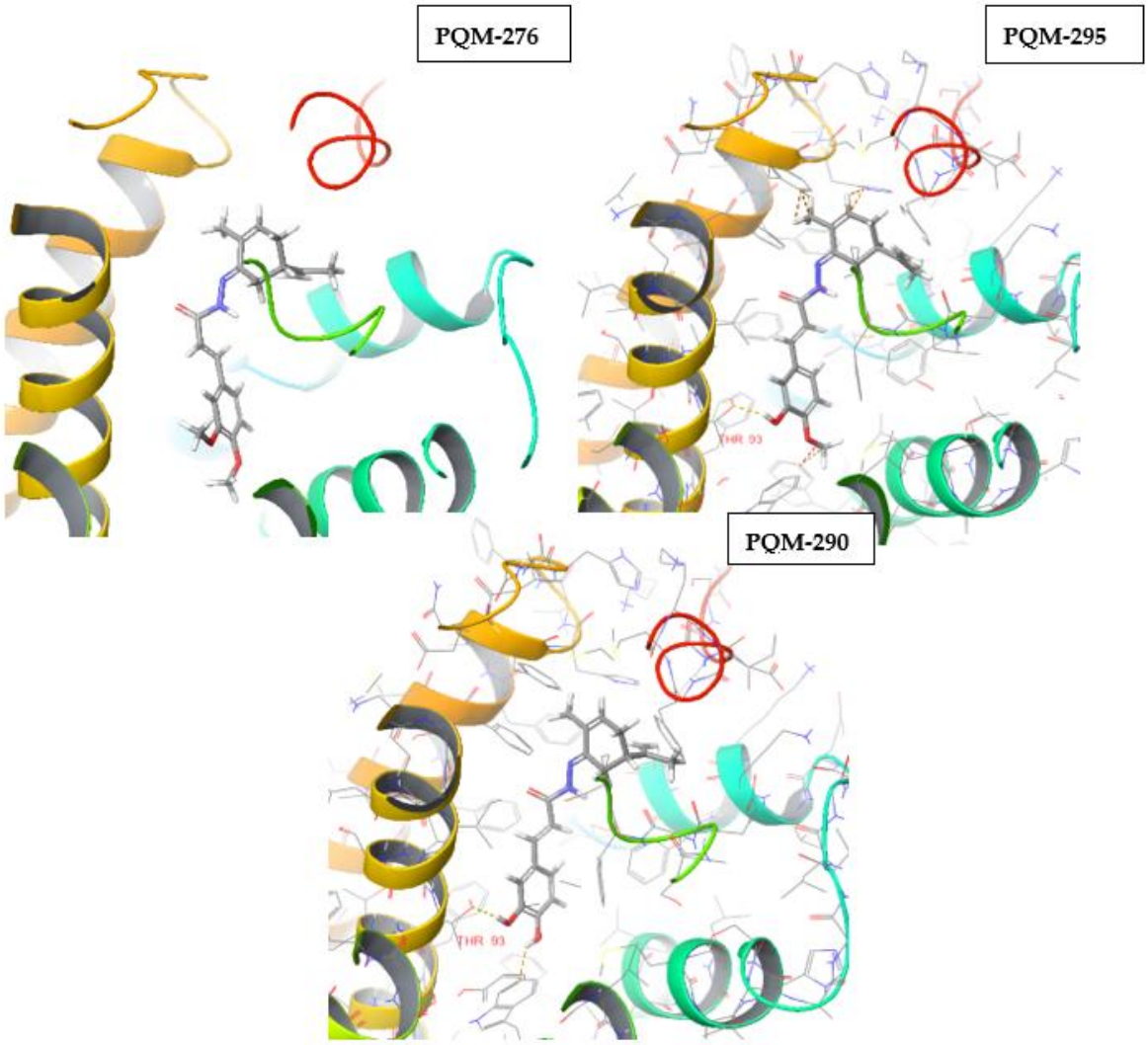


**Figure 8.** Predicted positions of PQM-276, PQM-295 and PQM-290 in the docking results for CB2 receptor, highlighting H-bond interactions of PQM-295 and PQM-290 with THR93 residue.

The evaluation of the binding affinity for the TRPV1 receptor, it was observed that all compounds were predicted with the terpene subunit facing the outside of the protein cavity, as exemplified by PQM-295 and PQM-376 in Figure 9. Once more, as observed for CB2, a few interactions were predicted for TRPV1, and none of these were predicted to interact with the structural residues THR550, SER512, ARG557, TYR511, LEU515, VAL518, MET547, ILE573, LEU669 located in the vanilloid site, which is described as responsible for the antinociceptive activity [28].

 doi:10.20944/preprints202504.2053.v1



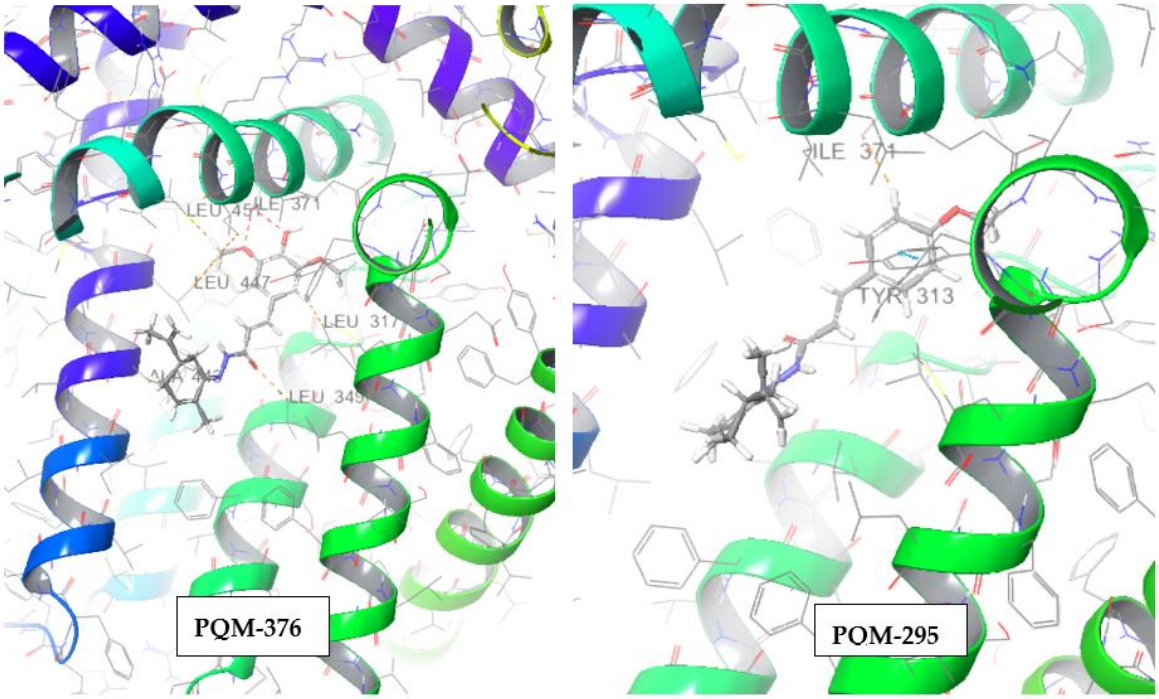


**Figure 9.** Predicted positions in the docking results for TRPV1 receptor related to PQM-376 and PQM-295.

It is worth mentioning that the molecular docking study can contribute to the understanding of the molecular affinity between the evaluated compounds and the selected targets, with *in vitro* and *in vivo* studies being necessary for a better discussion of the observed data.

*2.3. ADME Properties*

All compounds were evaluated *in silico* for their ADME properties by using the QikProp V.3.5 (Schrödinger) software. The five-top most active compounds PQM-292, PQM-293, PQM-295, PQM-307, PQM-308, and PQM-309 in the 1st phase of the formalin test, in the second phase (PQM-292), as well as PQM-274, PQM-291, PQM-294, PQM-304, PQM-305, and PQM-378, which exhibited the best results in the hot plate model, (all highlighted in Table 2) were predicted with moderate blood-brain barrier (BBB) permeability, but were predicted to be inactive in the CNS, similarly to CBD. In addition, QPPCaco values indicated good intestinal absorption, as well as moderate lipophilicity (QPlogPo/w), ability to bind human serum albumin (QPLogKHSA), and cellular permeability (MDCK cells). Despite all compounds seem to violate the Jorgensen's rule of 3, none of them showed violation number higher than 1 related to the Lipinski's rule, which could indicate moderate to good oral bioavailability and adequate drug-like properties for further development.

**Table 2.** *In silico* ADME prediction data for all series of synthetic compounds and CBD.

| *Cpd. PQM* | *CNS* | *HBD* | *HBA* | *QP logPo/w* | *QP logS* | *QP logHERG* | *QPP Caco* | *Q logBB* | *QPPMDCK* | *QPLog KHSA* | *% HOA* | *RO5* | *RO3* |
|---|---|---|---|---|---|---|---|---|---|---|---|---|---|
| *273* | -2 | 2 | 3.5 | 4.563 | -6.234 | -6.026 | 755.097 | -1.205 | 365.162 | 0.767 | 100 | 0 | 12 |
| ***274*** | **-2** | **2** | **3.5** | **4.563** | **-6.234** | **-6.026** | **755.097** | **-1.205** | **365.162** | **0.767** | **100** | **0** | **12** |
| *275* | 0 | 1 | 3.5 | 5.448 | -6.923 | -6.068 | 2309.278 | -0.659 | 1222.432 | 1.009 | 100 | 1 | 12 |
| *276* | 0 | 1 | 3.5 | 5.448 | -6.923 | -6.068 | 2309.458 | -0.659 | 1222.535 | 1.009 | 100 | 1 | 12 |

 doi:10.20944/preprints202504.2053.v1



| | | | | | | | | | | | | | |
|---|---|---|---|---|---|---|---|---|---|---|---|---|---|
| *290* | -2 | 3 | 3.5 | 3.656 | -5.546 | -6.04 | 249.314 | -1.739 | 110.231 | 0.505 | 91.251 | 0 | 12 |
| ***291*** | **-2** | **3** | **3.5** | **3.65** | **-5.514** | **-6.007** | **250.504** | **-1.729** | **110.8** | **0.503** | **91.251** | **0** | **12** |
| ***292*** | **-2** | **2** | **2.75** | **4.41** | **-5.979** | **-6.163** | **700.726** | **-1.157** | **336.826** | **0.734** | **100** | **0** | **12** |
| ***293*** | **-2** | **2** | **2.75** | **4.41** | **-5.979** | **-6.163** | **700.744** | **-1.157** | **336.836** | **0.734** | **100** | **0** | **12** |
| ***294*** | **0** | **1** | **2.75** | **5.33** | **-6.658** | **-6.172** | **2306.787** | **-0.582** | **1221.007** | **0.99** | **100** | **1** | **12** |
| ***295*** | **0** | **1** | **2.75** | **5.33** | **-6.658** | **-6.172** | **2306.514** | **-0.582** | **1220.851** | **0.99** | **100** | **1** | **12** |
| *300* | 0 | 1 | 2 | 6.229 | -7.886 | -6.223 | 2307.579 | -0.244 | 5393.733 | 1.249 | 100 | 1 | 12 |
| *301* | 0 | 1 | 2 | 6.227 | -7.884 | -6.225 | 2309.438 | -0.245 | 5369.953 | 1.248 | 100 | 1 | 12 |
| *302* | -2 | 2 | 2.75 | 4.462 | -5.917 | -6.168 | 853.249 | -1.053 | 416.727 | 0.725 | 100 | 0 | 12 |
| *303* | -2 | 2 | 2.75 | 4.456 | -5.901 | -6.155 | 854.156 | -1.051 | 417.205 | 0.722 | 100 | 0 | 12 |
| ***304*** | **0** | **1** | **3.5** | **4.754** | **-5.94** | **-5.775** | **2308.067** | **-0.484** | **1221.74** | **0.776** | **100** | **0** | **15** |
| ***305*** | **0** | **1** | **3.5** | **4.752** | **-5.934** | **-5.769** | **2306.555** | **-0.484** | **1220.874** | **0.775** | **100** | **0** | **15** |
| *306* | 0 | 1 | 2 | 5.723 | -7.16 | -6.183 | 2309.901 | -0.342 | 3014.466 | 1.095 | 100 | 1 | 12 |
| ***307*** | **0** | **1** | **2** | **5.726** | **-7.168** | **-6.19** | **2308.571** | **-0.343** | **3012.579** | **1.096** | **100** | **1** | **12** |
| ***308*** | **-2** | **2** | **3.5** | **4.537** | **-6.305** | **-6.097** | **697.894** | **-1.259** | **335.355** | **0.765** | **100** | **0** | **12** |
| ***309*** | **-2** | **2** | **3.5** | **4.537** | **-6.305** | **-6.097** | **697.895** | **-1.259** | **335.356** | **0.765** | **100** | **0** | **12** |
| *375* | -2 | 2 | 4.25 | 4.733 | -6.346 | -5.812 | 936.171 | -1.161 | 460.669 | 0.785 | 100 | 0 | 12 |
| *376* | -2 | 2 | 4.25 | 4.734 | -6.358 | -5.819 | 929.932 | -1.166 | 457.351 | 0.787 | 100 | 0 | 12 |
| *377* | 0 | 1 | 3 | 5.687 | -7.105 | -6.092 | 2466.783 | -0.551 | 1312.796 | 1.142 | 100 | 1 | 12 |
| ***378*** | **0** | **1** | **3** | **5.672** | **-7.122** | **-6.126** | **2473.389** | **-0.553** | **1316.596** | **1.135** | **100** | **1** | **12** |
| *379* | 0 | 1 | 2 | 5.233 | -6.223 | -6.129 | 2638.193 | -0.424 | 1411.668 | 0.958 | 100 | 1 | 12 |
| *380* | 0 | 1 | 2 | 5.229 | -6.234 | -6.146 | 2637.946 | -0.426 | 1411.525 | 0.957 | 100 | 1 | 12 |
| ***CBD*** | 0 | 2 | 1.5 | 5.025 | -5.519 | -4.892 | 2695.653 | -0.43 | 1444.93 | 0.883 | 100 | 1 | 1 |

**CNS-** Predict central nervous system activity (-2, inactive to +2, active). **HBD**-Hydrogen bonding donor (0 to 6). **HBA-**Hydrogen bonding acceptors (2 to 20). **QPlogP o/w**-Predicted octanol/water partition coefficient (-2.0 to 6.5). **QPlogS**-Aqueous solubility (-6.5 to 0.5). **QPlogHERG-** Predicted $IC_{50}$ value for blockage of HERG $K^+$ channels (concern below -5). **QPPCaco-**Permeability on cell assay, model for intestinal absorption (<25 poor; >500 good). **QPlogBB**-Permeability in the blood–brain barrier (-3.0 to 1.2). **QPPMDK-** Predicted apparent MDCK cell permeability in nm/sec. MDCK cells are considered to be a good mimic for the blood-barrier (<25 poor; >500 good). **QPLogKHSA-** Prediction of binding to human serum albumin (-1.5 to 1.5). **% HOA**-Percentage of human absorption by oral route (<25%-low; >80%-high in Caco). **RO5: rule of 5-** Number of violations of Lipinski's rule of 5; compounds that satisfy these rules are considered drug-like (Max.4). **RO3: rule of 3-** Number of

 doi:10.20944/preprints202504.2053.v1



violations of Jorgensen's rule; compounds with fewer violations of these rules are more likely to be orally available (Max. 3).3. Discussion.

In this work, to the best of our knowledge, we report for the first time a series of CBD-based *N*-acyl-hydrazones with potential antinociceptive and anti-inflammatory activity. Twenty-six compounds were synthesized in a two-step synthetic route from the natural monoterpene *R*- and *S*-carvones, coupled to diverse cinnamic acid-derived hydrazides, in moderate yields. All compounds were screened for their *in vivo* antinociceptive and anti-inflammatory effects at a fixed dose of 10 µmol/kg on the two classical formalin and hot plate models. In the neurogenic phase of the formalin test, it was evidenced PQM-292 (**11d**), PQM-293 (**10d**), PQM-295 (**10e**), PQM-307 (**10i**), PQM-308 (**11j**), and PQM-309 (**10j**) as the most active compounds, exhibiting a comparable antinociceptive profile as for morphine. Literature data suggest that treatment with CBD for chronic injury in mice or rats can be done with doses of 5 to 20 mg/kg [29–31], resulting in significant antinociceptive effects. Therefore, it seems to be clear that those six-aforementioned compounds, especially PQM-292 and PQM-293, demonstrated promising antinociceptive activity, surpassing CBD, and being comparable to morphine at a low dose. Notably, in the anti-inflammatory phase of the formalin assay [22], PQM-292 exhibited remarkable activity, showing better results than the control groups treated with morphine and ASA. Interestingly, studies investigating CBD's effect on inflammatory pain have demonstrated its antiallodynic effect at 2.5 mg/kg (*i.p.*), with no differences observed between male and female animals [32]. Thus, our results suggest that PQM-292 may act through a different mechanism of action than its analogues, exhibiting both antinociceptive and anti-inflammatory activities.

In the hot plate model, we observed that compounds PQM-274 (**11a**), PQM-291 (**10c**), PQM-294 (**11e**), PQM-304 (**11h**), PQM-305 (**10h**), and PQM-378 (**11l**) exhibited antinociceptive effects similar to those observed for the morphine-treated group. Notably, compound PQM-274 (**11a**) exhibited an almost equivalent effect to that of morphine. In literature, CBD has been reported to exhibit similar antinociceptive effect at doses of 3 and 30 mg/kg. On the other hand, considering that the hot plate model is based on an acute response to intense and short-term thermal stimuli, whereas formalin test involves induced persistent noxious stimulation, studies suggest that the type of pain model used can influence behavioral responses [33]. This could potentially explain the differences observed in the effect of the most active compounds in both animal models and it is reasonable to consider that these compounds could act through different mechanisms related to the modulation of TRPA1 receptor in the formalin test [34], and TRPV1 in the hot plate assay [35].

Regarding the possible molecular mechanisms underlying the antinociceptive activity of the target-compounds, it is known that CBD interacts directly and indirectly with the ECS, but with relative low affinity for CB1 and CB2. In comparison to CBD, the most active compounds in the series **10a-m**/**11a-m** were predicted to exhibit a slight affinity for CB1, even though neither of them showed significant interactions with structural residues associated to the antinociceptive effect [29]. Considering that TRPV1 channels are mainly expressed on unmyelinated C-fibers [30], which are required for the antiallodynic effect of CBD [29], docking studies were also performed to evaluate the binding affinity of the synthetic analogues with this receptor. However, our computational data did not demonstrate relevant interactions with structural residues that could corroborate the *in vivo* results, especially for PQM-292 (**11d**) that was the most active compound in both phases of the formalin test. It is possible to suppose that PQM-292 and its analogues could act through different mechanisms, maybe involving TRPA1 receptor, reinforcing the need for further detailed studies.

Considering the *in vivo* results and the computational data, a structure-activity relationship analysis suggested that stereochemistry of the terpene moiety is not crucial for biological activity and does not influence the docking position of the ligands at the protein cavity on CB1, CB2 or TRPV1 receptors. On the other hand, the presence of methoxy or dialkylamine groups, rather than H-bond donors such as hydroxyl substituents on the aromatic ring appears to induce a similar orientation of the ligands within the CB1 cavity. Additionally, hydroxy substituents at the C3, C4 or C5 positions

 doi:10.20944/preprints202504.2053.v1



were observed to favor a conformational change in which the terpene moiety twists to the opposite side compared to other analogues. Moreover, the hydroxyl group at the C3 position, when present as the sole substituent in the aromatic ring, was found to be crucial for enhancing antinociceptive activity, as seen in the most active compound, PQM-292.

## 4. Materials and Methods

### *4.1. ADME Properties*

Methods NMR spectra were obtained from a BRUKER AVANCE DRX 300 MHz spectrometer. IR spectra were generated in a Nicolet iS50 FTIR (Thermo Scientific, USA) spectrometer, coupled with Pike Gladi ATR Technologies. $^{1}H$ (300 MHz) and $^{13}C$ (75 MHz) NMR chemical analyses were reported in parts per million ($\delta$) relative to tetramethylsilane (0.00 ppm) or other deuterated solvent ($CDCl_3$ or DMSO-*d6*) as an internal standard. Coupling constants (*J*) were reported in hertz (Hz) and were obtained by MestreReNova software. Abbreviations of multiplicity were as follows: s: singlet, d: doublet, t: triplet, q: quartet, m: multiplet. Data were presented as: multiplicity, integration, coupling constant. Analytical thin layer chromatography (TLC) experiments were performed on Merck silica gel 60 F254 plates, eluted in hexane/ethyl acetate in concentration gradient, and visualized under UV light (256 nm) or chemical reaction (e.g. $I_2$). Normal-phase column chromatography was performed on Sigma-Aldrich silica gel or in Isolera automatic chromatograph (Biotage). The commercial substituted cinnamic acids, *R*- and *S*-carvone were without further purification. The solvents were treated and distilled by conventional methods.

4.1.1. Synthesis of Hydrazide Intermediates (8a-m)

A solution of the correspondent cinnamic acid (7a-m, 1.0 eq) in acetonitrile, MeCN. Hydrochloride (1,2 eq) and HOBt (1,2 eq) diluted with MeCN was added, and the mixture was stirred at room temperature for 1 hour and a half, with precipitate formation. Right away, hydrazine monohydrate (10 eq) diluted in MeCN (at 0°C) slowly dripped in the initial solution. The reaction was stirred at room temperature for 45 minutes. Solvent was removed under pressure, then $NaHCO_3$ 10% (2 mL) was added, to precipitate the formed product, which was filtrated with distilled $H_2O$. The products obtained were pale yellow or white solids, with a yield of 20-100%.

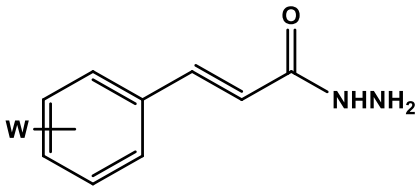


**(*E*)-3-(4-hydroxy-3-methoxyphenyl) acrylohydrazide (8a)**
**MW:** 208.21 g/mol. **Chemical Formula:** $C_{10}H_{12}N_2O_3$. **Physical appearance:** yellow solid. **yield:** 53%. **IR** (ATR,$\upsilon_{max}$, $cm^{-1}$): 3278 e 3202 ($\nu_{as/s}$ R-$NH_2$), 1655 ($\nu$ RHC=CHR), 1585 ($\nu$ C=O), 1518 ($\delta$ NH), 1466 e 1427 ($\delta_{as/s}$ $CH_3$), 1033 ($\nu$ Ar-O-C), 961 ($\delta$RHC=CHR), 835 e 810 ($\delta$ C-$H_{ar}$), 714 ($\delta$NH). **$^{1}H$ NMR** (300 MHz, DMSO-$d_6$), $\delta$ (ppm): 9.47 (s, 1H, H11), 9.20 (s, 1H, H12), 7.34 (d, *J*= 15.7 Hz, 1H, H7), 7.11 (s, 1H, H5), 6.99 (d, *J*= 9.8 Hz, 1H, H1), 6.78 (d, *J*= 8.1 Hz, 1H, H2), 6.36 (d, *J*= 15.7 Hz, 1H, H8), 4.41 (s, 2H, H13), 3.79 (s, 3H, H10); **$^{13}C$ NMR** (75 MHz, DMSO-$d_6$) $\delta$ (ppm): 165.6 (C9), 148.7 (C3), 148.3 (C4), 139.1 (C7), 126.8 (C6), 121.8 (C1), 117.3 (C8), 116.1 (C2), 111.3 (C5), 56.0 (C10).

**(*E*)-3-(3,4-dimethoxyphenyl)acrylohydrazide (8b)**
**MW:** 222.24 g/mol. **Chemical Formula:** $C_{11}H_{14}N_2O_3$. **Physical appearance:** yellow solid. **yield:** 77%. **IR** (ATR, $\upsilon_{max}$, $cm^{-1}$): 3322 and

 doi:10.20944/preprints202504.2053.v1



3228 ($\nu_{as/s}$ R-$NH_2$), 3013 ($\nu$ =CH), 2996 ($\nu_{as}$ $CH_3$), 1660 ($\nu$ C=C), 1651 ($\nu$ C=O), 1506 ($\delta$ NH), 1464 and 1452 ($\delta$ $CH_3$), 1259 ($\nu_{as}$ =Ar-O-C), 1016 ($\nu_{as}$ Ar-O-C), 964 ($\delta$ CH). **$^1$H NMR** (300 MHz, DMSO-*d*$_6$), $\delta$ (ppm): 9.27 (s, 1H), 7,38 (d, *J*= 15.8 Hz, 1H, H7), 7.14 (d, *J*= 1.9 Hz, 1H, H5), 7.11 (dd, *J*= 8.35 Hz, *J*= 1.9 Hz, 1H, H1), 6.97 (d, *J*= 15.8 Hz, 1H, H2), 6.44 (d, *J*= 15.77 Hz, 1H, H8), 4.42 (s, 2H, H13), 3.78 (s, 3H, H11), 3.77 (s, 3H, H10); **$^{13}$C NMR** (75 MHz, DMSO-*d*$_6$) $\delta$ (ppm): 165.4 (C9), 150.2 (C4), 149.4 (C3), 138.8 (C7), 128.2 (C6), 121.7 (C8), 118.4 (C1), 112.2 (C2), 110.6 (C5), 56.0 (C10/11).

**(*E*)-3-(3,4-dihydroxyphenyl)acrylohydrazide (8c)**

**MW:** 194.19 g/mol. **Chemical Formula:** $C_9H_{10}N_2O_3$. **Physical appearance:** yellow solid. **yield:** 20%. **IR** (ATR, $\upsilon_{max}$, $cm^{-1}$): 3446 ($\nu$ OH), 3341 and 3312 ($\nu_{as/s}$ $NH_2$), 2928 and 2867 ($\nu_{as/s}$ CH), 1688 ($\nu$ C=O), 1637 ($\nu$ C=C), 1590 ($\delta$ NH), 1258 ($\delta$ OH), 1037 ($\nu$ C-OH). **$^1$H NMR** (300 MHz, DMSO-*d*$_6$), $\delta$ (ppm): 9.2 (s, 1H, H12); 7.25 (d, *J*= 15.7 Hz, 1H, H7), 6.93 (d, *J*= 1.74 Hz, 1H, H5), 6.82 (dd, *J*= 8.1 Hz, *J*= 1.75 Hz, 1H, H1), 6.73 (d, *J*= 8.1 Hz, 1H, H2), 6.24 (d, *J*= 15.7 Hz, 1H, H8), 4.37 (s, 2H, H13); **$^{13}$C NMR** (75 MHz, DMSO-*d*$_6$) $\delta$ (ppm): 165.1 (C5), 147.3 (C11), 145.6 (C10), 138.7 (C7), 126.3 (C6), 120.4 (C8), 116.4 (C1), 115.7 (C2), 113.6 (C5).

**(*E*)-3-(4-hydroxyphenyl)acrylohydrazide (8d)**

**MW:** 178.19 g/mol. **Chemical Formula:** $C_9H_{10}N_2O_2$. **Physical appearance:** yellow solid. **yield:** 27%. **IR** (ATR, $\upsilon_{max}$, $cm^{-1}$): 3325 and 3269 ($\nu_{as/s}$ $NH_2$), 3196 ($\nu$ CH), 1654 ($\nu$ C=C), 1608 ($\nu$ C=O), 1511 ($\delta$ NH), 1035 ($\nu$ C-OH), 825 ($\delta$ C-H ar. 1,4 dissubstituted). **$^1$H NMR** (300 MHz, DMSO-*d*$_6$) $\delta$ (ppm): 9.21 (s, 1H, H11), 7.38 (d, *J*= 8.6 Hz ,2H, H1; H5), 7.31 (s, 1H, H7), 6.78 (d, *J*= 8.60 Hz 2H, H2; H4), 4.40 (s, 2H, H12); **$^{13}$C NMR (**75 MHz, DMSO-*d*$_6$) $\delta$ (ppm): 165.2 (C9), 158.9 (C10), 138.4 (C7), 129.2 (C1/5), 126.6 (d, *J* = 15.8Hz, 1H, H8), 116.7 (C8), 115.8 (C2/4).

**(*E*)-3-(4-methoxyphenyl)acrylohydrazide (8e)**

**MW:** 192.21 g/mol. **Chemical Formula:** $C_{10}H_{12}N_2O_2$. **Physical appearance:** white solid. **yield:** 59%. **IR** (ATR, $\upsilon_{max}$, $cm^{-1}$): 3309 and 3278 ($\nu_{as/s}$ $NH_2$), 3012 ($\nu$ =CH-), 2952 e 2835 ($\nu_{as/s}$ $CH_3$), 1655 ($\nu$ C=C), 1602 ($\nu$ C=O), 1521 ($\delta$ NH), 1462 e 1441 ($\delta_{as/s}$ $CH_3$), 965 ($\delta$ =CH) 820 ($\delta$ $CH_{ar}$). **$^1$H NMR** (300 MHz, $CDCl_3$) $\delta$ (ppm): 7.64 (d, *J*= 15.6 Hz, 1H, H7), 7.50 (s, 1H, H11), 7.42-7.47 (m, 2H, H1;H5), 6.86-6.90 (m, 2H, H2;H4), 6.23 (d, *J*= 15.6 Hz, 1H, H8), 3.82 (s, 3H, H10); **$^{13}$C NMR** (75 MHz, $CDCl_3$) $\delta$ (ppm): 167.5 (C9), 161.1(C3), 141.5 (C7), 129.5 (C1/5), 127.3 (C6), 115.3 (C8), 114.3 (C2/4), 55.4 (C10).

**(*E*)-3-(4-(trifluoromethyl)phenyl)acrylohydrazide (8f)**

**MW:** 230.19 g/mol. **Chemical Formula:** $C_{10}H_9F_3N_2O$. **Physical appearance:** white solid. **yield:** 70%. **IR** (ATR, $\upsilon_{max}$, $cm^{-1}$): 3441 and 3213 ($\nu_{as/s}$ $NH_2$), 3316 ($\nu$ NH), 1646 ($\nu$ C=C), 1610 ($\nu$ C=O), 1531 ($\delta$ NH), 1317 ($\nu$ $CF_3$), 836 ($\delta$ $CH_{ar}$). **$^1$H NMR** (300 MHz, DMSO-*d*$_6$) $\delta$ (ppm): 7.76 (s, 4H, H1;H2;H4;H5), 7.51 (d, *J*= 15.9 Hz, 1H, H7), 6.67 (d, *J*= 15.9 Hz, 1H, H8), 4.55 (s, 2H, H12); **$^{13}$C NMR** (75 MHz, DMSO-*d*$_6$) $\delta$ (ppm): 163.8 (C9), 139.0 (C7), 136.6 (C6), 128.1 (C1/2/4/5), 125.8 (C3), 123.1 (C8).

**(*E*)-3-(2-hydroxyphenyl)acrylohydrazide (8g)**

**MW:** 178.19 g/mol. **Chemical Formula:** $C_9H_{10}N_2O_2$. **Physical appearance:** brown solid. **yield:** 73%. **IR** (ATR, $\upsilon_{max}$, $cm^{-1}$): 3324 and 3296 ($\nu_{as/s}$ $NH_2$), 3173 ($\nu$ NH), 3059 and 2969 ($\nu$ CH), 1643 ($\nu$ C=O), 1585 ($\delta$ $NH_2$), 1526 ($\delta$ NH), 1343 and 1255 ($\delta$ OH + $\nu$ =C-O), 760 ($\delta$ $CH_{ar}$). **$^1$H**

 doi:10.20944/preprints202504.2053.v1



**NMR** (300 MHz, DMSO-$d_6$) $\delta$ (ppm): 9.29 (s, 1H, H11), 7.64 (d, *J*= 15.9 Hz, 1H, H7), 7.40 (d, *J*= 7.55 Hz, *J*= 1.5 Hz, 1H, H1), 7.16 (t, 1H, H3), 6.88 (d, *J*= 8.1 Hz, 1H, H4), 6.88 (d, *J*= 8.1 Hz, 1H, H2), 6.59 (d, *J*= 15.9 Hz, H8), 4.41 (s, 2H, H12); **$^{13}$C (**75 MHz, DMSO-$d_6$) $\delta$ (ppm): 165.3 (C9), 156.3 (C1), 134.2 (C7), 130.4 (C4), 128.2 (C2), 121.7 (C6), 119.7 (C8), 119.3 (C5), 116.1 (C3).

**(*E*)-3-(benzo[d][1,3]dioxol-5-yl)acrylohydrazide (8h)**

**MW:** 206.20 g/mol. **Chemical Formula:** $C_{10}H_{10}N_2O_3$. **Physical appearance:** brown solid. **yield:** 59%. **IR** (ATR, $\upsilon_{max}$, $cm^{-1}$): 3314 (νNH), 3033 (ν =CH), 1661 (ν C=C), 1608 (ν C=O), 1450 ($\delta_s$ $CH_2$), 1258 ($\nu_{as}$ C-O-C), 924 ($\delta$ $CH_2$). **$^1$H NMR** (300 MHz, DMSO-$d_6$) $\delta$ (ppm): 9.25 (s, 1H, H11), 7.35 (d, *J*= 15.75 Hz, 1H, H7), 7.13 (d, *J*= 1.4 Hz, 1H, H5), 7.06 (dd, *J*= 8.1 Hz, *J*= 1.4 Hz, 1H, H1), 6.94 (d, *J*= 8.1 Hz, 1H, H4), 6.38 (d, *J*= 15.75 Hz, 1H, H8), 6.05 (s, 2H, H10), 4.42 (s, 2H, H12); **$^{13}$C** (75 MHz, DMSO-$d_6$) $\delta$ (ppm): 164.8 (C9), 148.4 (C3), 148.0 (C2), 138.0 (C7), 129.3, (C6), 123.2 (C1), 118.4 (C8), 108.6 (C5), 106.2 (C4), 101.5 (C10).

**(*E*)-3-(4-chlorophenyl)acrylohydrazide (8i)**

**MW:** 196.63 g/mol. **Chemical Formula:** $C_9H_9ClN_2O$. **Physical appearance:** white solid. **yield:** 100%. **IR** (ATR, $\upsilon_{max}$, $cm^{-1}$): 3274 (ν $NH_2$), 3034 (ν =CH), 1661 (νC=C), 1629 (ν C=O), 1558 ($\delta$ NH), 1035 (C-Cl), 969 ($\delta$ HC=CH) 819 ($\delta$ $CH_{ar}$). **$^1$H NMR** (300 MHz, DMSO-$d_6$) $\delta$ (ppm): 9.52 (s, 1H, H11), 7.56-7.60 (m, 2H, H1/5), 7.45-7.48 (m, 2H, H2/4), 7.40 (s, 1H, H7), 6.55 (d, *J* = 15.9 Hz, 1H, H8); **$^{13}$C NMR** (75 MHz, DMSO-$d_6$) $\delta$ (ppm): 164.2 (C9), 136.8 (C7), 134.3 (C3/C6), 129.6 (C1/5), 129.4 (C2/4), 121.1 (C8).

**(*E*)-3-(3-hydroxy-4-methoxyphenyl)acrylohydrazide (8j)**

**MW:** 208.21 g/mol. **Chemical Formula:** $C_{10}H_{12}N_2O_3$. **Physical appearance:** yellow solid. **yield:** 75%. **IR** (ATR, $\upsilon_{max}$, $cm^{-1}$): 3333 (νNH$_2$), 3154 (ν NH),1651 (ν C=O), 1594 ($\delta$ NH), 1495 (ν C=C$_{ar}$), 1443 and 1364 ($\delta$ $CH_3$), 995 ($\delta$ HC=CH). **$^1$H NMR** (300 MHz, DMSO-$d_6$) $\delta$ (ppm): 9.26 (s, 1H, H10), 9.23 (s, 1H, H12), 7.30 (d, *J*= 15.74 Hz, 1H, H7), 6.98 (s, 1H, H5), 6.90-6.94 (m, 2H, H2; H1), 6.31 (d, *J*= 15.74 Hz, 1H, H8), 4.43 (s, 2H, H13), 3.78 (s, 3H, H11); **$^{13}$C NMR (**75 MHz, DMSO-$d_6$) $\delta$ (ppm): 165.2 (C9), 149.4 (C10), 146.9 (C3), 138.6 (C7), 128.0 (C6), 120.6 (C1), 117.8 (C8), 113.4 (C2), 112.3 (C5), 58.2 (C11).

**(*E*)-3-(4-hydroxy-3,5-dimethoxyphenyl)acrylohydrazide (8k)**

**MW:** 238.24 g/mol. **Chemical Formula:** $C_{11}H_{14}N_2O_4$. **Physical appearance:** yellow solid. **yield:** 62%. **IR** (ATR, $\upsilon_{max}$, $cm^{-1}$): 3333 (νNH$_2$), 3154 (ν NH), 1651 (ν C=O), 1594 ($\delta$ NH), 1495 (ν C=C$_{ar}$), 1443 and 1364 ($\delta$ $CH_3$), 995 ($\delta$ HC=CH). **$^1$H NMR** (300 MHz, DMSO-$d_6$) $\delta$ (ppm): 9.18 (s, 1H, H13), 7.35 (d, *J*= 15.7 Hz, 1H, H7), 6.83 (s, 2H, H1; H5), 6,40 (d, *J*= 15.7 Hz, 1H, H8), 4.40 (s, 2H, H14), 3.78 (s, 6H, H10; H12); **$^{13}$C NMR** (75 MHz, DMSO-$d_6$) $\delta$ (ppm): 165.1 (C9), 148.1 (C2/C4), 139.0 (C7), 137.3 (C3), 125.2 (C6), 117.3 (C8), 105.3 (C1/C5), 56.0 (C10/C12),

**(*E*)-3-(4-(dimethylamino)phenyl)acrylohydrazide (8l)**

**MW:** 205.26 g/mol. **Chemical Formula:** $C_{11}H_{15}N_3O$. **Physical appearance:** yellow solid. **yield:** 100%. **IR** (ATR, $\upsilon_{max}$, $cm^{-1}$): 3333 (νNH$_2$), 3154 (ν NH),1651 (ν C=O), 1594 ($\delta$ NH), 1495 (ν C=C$_{ar}$), 1443 and 1364 ($\delta$ $CH_3$), 995 ($\delta$ HC=CH). **$^1$H NMR** (300 MHz, C*D*Cl$_3$) $\delta$ (ppm): 7.61 (d, *J*= 15.4 Hz, 1H, H7), 7.40 (d, *J*= 8.7 Hz, 2H, H1; H5), 6.99 (s, 1H, H11), 6.66 (d, *J*= 8.7 Hz, 2H, H2; H4), 6.15 (d, *J* = 15.4 Hz, 1H, H8), 3.00

 doi:10.20944/preprints202504.2053.v1



(s, 6H, H10); **$^{13}$C NMR** (75 MHz, C*D*Cl$_3$) $\delta$ (ppm): 168.2 (C9), 151.6 (C3), 142.2 (C7), 129.4 (C1/C5), 122.4 (C6), 112.4 (C8), 111.9 (C2/C4), 40.2 (C10).

**Cinnamoylhydrazide (8m)**

**MW:** 162.19 g/mol **Chemical Formula:** $C_9H_{10}N_2O$ **Physical appearance:** white solid. **yield:** 73%. **IR** (ATR, $\upsilon_{max}$, cm$^{-1}$): 3333 ($\nu NH_2$), 3154 ($\nu$ NH),1651 ($\nu$ C=O), 1594 ($\delta$ NH), 1495 ($\nu$ C=C$_{ar}$), 1443 and 1364 ($\delta$ CH$_3$), 995 ($\delta$ HC=CH). **$^1$H NMR** (300 MHz, C*D*Cl$_3$) $\delta$ (ppm): 8.78 (s, 1H, H10), 7.80 (d, *J*= 15.9, 1H, H7), 7.31-7.61 (m, 6H, H1, H2, H3, H4, H5 e H8); **$^{13}$C NMR** (75 MHz, C*D*Cl$_3$) $\delta$ (ppm): 167.3 (C9), 143.4 (C7), 132.3 (C6), 129.9 (C3), 128.8 (C2/C4), 128.3 (C1/C5), 116.9 (C8).

4.1.2. Synthesis of terpene-cinnamoyl-N-acyl-hydrazones (10a-m and 11a-m)

Freshly distilled R- or S-carvones (1 eq.) were diluted in anhydrous MeOH and stirred for 2 minutes, followed by addition of glacial AcOH (10-15 drops). Next, a solution of the correspondent hydrazide intermediates (8a-m,1 eq.) in dry MeOH was added to the reaction flask, and the reaction was maintained under stirring and room temperature, and the reaction was finished when TLC analysis showed the total consumption of the starting material. The reaction mixture was concentrated low pressure, and the solid material was filtered and/or precipitated with ice-cold MeOH, followed by washing with cold-water and cold-MeOH to remove the unreacted carvone amount. The purified products were obtained as solids in 17-79% yields.

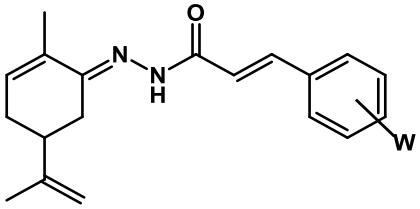


**(*E*)-3-(4-hydroxy-3-methoxyphenyl)-*N*'-((*R*,*E*)-2-methyl-5-(prop-1-en-2-yl)cyclohex-2-en-1-ylidene)acrylohydrazide (PQM-273, 10a)**

**MW:** 340.42 g/mol. **Chemical Formula:** $C_{20}H_{24}N_2O_3$. **Physical appearance:** pale yellow solid. **Melting range**: 215-216°C. **Purity:** 100% (HPLC). Y**ield:** 18%. **IR** (ATR, νmax, cm$^{-1}$): 3280 (ν NH), 3055 ($\nu_{as}$ CH$_2$), 2969 ($\nu_s$ CH$_2$ ou $\nu_{as}$ CH$_3$), 2919 ($\nu_s$ CH$_2$), 2834 ($\nu_s$ CH$_3$), 1661 (ν C=O), 1635 (C=N), 1515 ($\delta$ NH), 1251 ($\nu_{as}$ Ar-O-C), 1028 ($\nu_s$ Ar-O-C), 978 ($\delta$ C-H). **$^1$H NMR** (300 MHz, CDCl$_3$), $\delta$ (ppm): 8.73 (s, 1H, H12), 7.75 (d, *J* = 15.9 Hz, 1H, H7), 7.40 (d, *J* = 15.9 Hz, 1H, H8), 7.17 (d, *J* = 6.92 Hz, 1H, H16), 7.08 (s, 1H, H5), 6.92 (d, *J* = 8.14 Hz, 1H, H2), 6.16 (d, *J* = 8.14 Hz, 1H, H15), 5.92 (s, 1H, H11), 4.82 (d, *J* = 13.0 Hz, 2H, H20), 3.93 (s, 3H, H10), 2.74 (dd, *J*= 4.0 Hz, *J*= 15.3 Hz 1H, H17), 2.29-2.45 (m, 2H, H17; H16), 2.07-2.18 (m, 2H, H18; H16), 1.97 (s, 3H, H21), 1.78 (s, 3H, H22); **$^{13}$C NMR** (75 MHz, CDCl$_3$), $\delta$ (ppm): 167.8 (C9), 149.2 (C13), 147.7 (C3), 147.3 (C4), 146.6 (C19), 143.5 (C7), 133.0 (C15), 132.7 (C14), 127.9 (C6), 122.6 (C1), 114.7 (C2), 114.2 (C8), 110.4 (C20), 110.1 (C5), 55.9 (C10), 40.6 (C17), 30.0 (C18), 28.5 (C16), 20.8 (C22), 17.8 (C21). *m*/*z* (Rel. Int.): 341.18571.

**(*E*)-3-(4-hydroxy-3-methoxyphenyl)-*N*'-((*S*,*E*)-2-methyl-5-(prop-1-en-2-yl)cyclohex-2-en-1-ylidene)acrylohydrazide (PQM-274, 11a)**

**MW:** 340.42 g/mol. **Chemical Formula:** $C_{20}H_{24}N_2O_3$. **Physical appearance:** yellow solid. **Melting range**: 209-201°C. **Purity (HPLC):** 100%. **Yield:** 57%. **IR** (ATR, νmax, cm$^{-1}$): 3274 (ν NH), 2967 ($\nu_s$ =CH$_2$ ou $\nu_{as}$ CH$_3$), 2918 ($\nu_s$ =CH$_2$), 1654 (ν C=O), 1616 (C=N), 1588 ($\delta$ NH), 1508 (ν C=C$_{ar}$)1270 ($\nu_{as}$ A-O-C), 1030 ($\nu_s$ Ar-O-C). **$^1$H NMR** (300 MHz, CDCl$_3$), $\delta$ (ppm): 9.24 (s, 1H, H12), 7.74 (d, *J*= 15.9 Hz, 1H, H7), 7.42 (d, *J*= 15.9 Hz, 1H, H8), 7.16 (dd, *J*= 8.2 Hz, *J*= 1.4 Hz, 1H, H16), 7.08 (d, *J*= 1.4 Hz, 1H, H5), 6.94 (d, *J*= 8.2 Hz, 1H, H2), 6.16 (d, *J*= 5.2 Hz, 1H, H15), 6.06, (s, 1H, H11), 4.83 (d, *J*= 4.3 Hz, 2H, H20), 3.93 (s, 3H, H10), 2.83 (dd, *J*= 3.4 Hz, *J*= 16.1 Hz, 1H, H18), 2.45 (dt, *J*= 4.0 Hz, *J*= 11.9 Hz 1H, H17), 2.33

 doi:10.20944/preprints202504.2053.v1



(dt, *J*= 5.0 Hz, *J*= 17.0 Hz 1H, H16), 2.05-2.19 (m, 2H, H18; H16), 1.97 (s, 3H, H21), 1.79 (s, 3H, H22); **$^{13}$C NMR** (75 MHz, $CDCl_3$), δ (ppm): 167.8 (C9), 149.5 (C13), 147.7 (C3), 147.4 (C4), 146.6 (C19), 143.4 (C7), 133.0 (C15), 132.7 (C14), 127.9 (C6), 122.6 (C1), 114.8 (C2), 114.3 (C8), 110.4 (C20), 110.1 (C5), 55.9 (C10), 40.6 (C17), 30.1 (C18), 28.7 (C16), 20.8 (C22), 17.8 (C21). *m*/*z* (Rel. Int.): 341.18582.

**(*E*)-3-(3,4-dimethoxyphenyl)-*N*'-((*R*,*E*)-2-methyl-5-(prop-1-en-2-yl)cyclohex-2-en-1-ylidene)acrylohydrazide (PQM-275, 10b)**

**MW:** 354.45 g/mol. **Chemical Formula:** $C_{21}H_{26}N_2O_3$. **Physical appearance:** pale yellow solid. **Melting range**: 246-248°C. **Purity (HPLC):** 100%. **Yield:** 71%. **IR** (ATR, vmax, $cm^{-1}$): 3158 (ν NH), 3063 ($\nu_{as}$ $CH_2$), 2988 ($\nu_s$ $CH_2$ ou $\nu_{as}$ $CH_3$), 2907 ($\nu_s$ $CH_2$), 2834 ($\nu_s$ $CH_3$), 1659 (ν C=O), 1594 (δ NH), 1518 (ν C=$C_{ar}$), 1463 e 1443 ($\delta_{as/s}$ $CH_3$), 1253 ($\nu_{as}$ Ar-O-C), 1023 ($\nu_s$ Ar-O-C), 980 (δ C-H). **$^1$H NMR** (300 MHz, $CDCl_3$), δ (ppm): 9.36 (s, 1H, H12), 7.76 (d, *J*= 15.9 Hz, 1H, H7), 7.46 (d, *J*= 15.9 Hz, 1H, H8), 7.18 (d, *J*= 8.3 Hz, 1H, H1), 7.13 (s, 1H, H5), 6.89 (d, *J*= 8.3 Hz, 1H, H2), 6.16 (d, *J*= 5.3 Hz, 1H, H15), 4.84 (s, 2H, H20), 3.93 (s, 6H, H11;H10), 2.87 (d, *J*= 14.1 Hz, 1H, H18), 2.41 (dt, *J*= 9.2 Hz, *J*= 7.7 Hz 1H, H17), 2.29-2.32 (m, 1H, H16), 2.11-2.18 (m, 2H, H18; H16), 1.97 (s, 3H, H21), 1.80 (s, 3H, H20); **$^{13}$C NMR** (75 MHz, $CDCl_3$), δ (ppm): 168.0 (C9), 150.8 (C3), 149.5 (C13), 149.1 (C4), 143.1 (C7), 133.0 (C14), 132.8 (C15), 128.4 (C6), 122.3 (C1), 114.7 (C2), 111.0 (C8), 110.4 (C5), 110.0 (C20), 56.0 (C11), 55.8 (C10), 40.6 (C17), 30.1 (C18), 28.8 (C16), 20.9 (C20), 17.8 (C21). *m*/*z* (Rel. Int.): 355.20161.

**(*E*)-3-(3,4-dimethoxyphenyl)-*N*'-((*S*,*E*)-2-methyl-5-(prop-1-en-2-yl)cyclohex-2-en-1-ylidene)acrylohydrazide (PQM-276, 11b)**

**MW:** 354.45 g/mol. **Chemical Formula:** $C_{21}H_{26}N_2O_3$. **Physical appearance:** pale yellow solid. **Melting range**: 239-240°C. **Purity (HPLC)**: 100%. **Yield:** 83%. **IR** (ATR, ν max, cm-1): 3158 (ν NH), 3063 ($\nu_{as}$ $CH_2$), 2988 ($\nu_s$ $CH_2$ ou $\nu_{as}$ $CH_3$), 2907 ($\nu_s$ $CH_2$), 2834 ($\nu_s$ $CH_3$), 1660 (ν C=O), 1615 (ν C=N), 1595 (δ NH), 1518 (ν C=$C_{ar}$), 1463 and 1443 ($\delta_{as/s}$ $CH_3$), 1253 ($\nu_{as}$ Ar-O-C), 1023 ($\nu_s$ Ar-O-C), 981 (δ C-H). **$^1$H NMR** (300 MHz, $CDCl_3$), δ (ppm): 9.48 (s, 1H, H12), 7.75 (d, *J*= 15.9 Hz, 1H, H7), 7.46 (d, *J*= 15.9 Hz, 1H, H8), 7.18 (d, *J*= 8.2 Hz, 1H, H1), 7.13 (s, 1H, H5), 6.89 (d, *J*= 8.2 Hz, 1H, H2), 6.16 (d, *J*= 4.1 Hz, 1H, H15), 4.85 (s, 2H, H20), 3.93 (s, 6H, H10; H11), 2.88 (dd, *J*= 15.9 Hz, *J*= 3.1 Hz, 1H, H18), 2.45 (t, *J*= 11.9 Hz, 1H, H17), 2.34 (dd, *J*= 18.0 Hz, *J*= 5.0 Hz , 1H, H16), 2.12 (dd, *J*= 15.0 Hz, *J*= 13.4 Hz 2H, H18; H16), 1.97 (s, 3H, H21), 1.81 (s, 3H, H20); **$^{13}$C NMR** (75 MHz, $CDCl_3$), δ (ppm): 168.0 (C9), 150.8 (C3), 149.6 (C13), 149.0 (C4), 143.1 (C7), 133.0 (C14), 132.8 (C15), 128.4 (C6), 122.3 (C1), 114.7 (C2), 111.0 (C8), 110.4 (C5), 110.0 (C20), 56.0 (C11), 55.8 (C10), 40.6 (C17), 30.1 (C18), 28.8 (C16), 20.9 (C20), 17.8 (C21). *m*/*z* (Rel. Int.): 355.20167.

**(*E*)-3-(3,4-dihydroxyphenyl)-*N*'-((*S*,*E*)-2-methyl-5-(prop-1-en-2-yl)cyclohex-2-en-1-ylidene)acrylohydrazide (PQM-290, 11c)**

**MW:** 326.40 g/mol. **Chemical Formula:** $C_{19}H_{22}N_2O_3$. **Physical appearance:** pale yellow solid. **Melting range**: 195-197ºC. **Purity (HPLC)**: 100%. **Yield:** 28%. **IR** (ATR, $\nu_{max}$, $cm^{-1}$): 3300 (ν OH), 3244 (ν NH), 1648 (ν C=O), 1616 (ν C=N), 1603 (δ NH), 1514 (ν C=$C_{ar}$), 1371 e 1120 (δ OH and ν =C-O), 979 (δ C=$CH_2$), 817 (δ RC=CH). **$^1$H NMR** (300 MHz, DMSO-$d_6$), δ (ppm): 10.45-10.41 (s, 1H, H12), 7.37 (dt, *J*= 16.0 Hz *J*= 30.08 Hz, 1H, H7), 7.02 (d, *J*= 13.2 Hz, 1H, H5), 6.91 (t, *J*= 6.8 Hz 1H, H1), 6.73 (dd, *J*= 11.9 Hz and *J*= 16.0 Hz, 2H, H2 e H8), 6.15 (s, 1H, H15), 4.80 (t, *J*= 7.7 Hz, 2H, H20), 2.92 (t, *J*= 12.7 Hz, 1H, H18), 2.21-2.36 (m, 2H, H17; H16), 2.01-2.14 (m, 2H, H18; H16), 1.91-1.83 (s, 3H, H22), 1.76 (s, 3H, H21); **$^{13}$C** (75 MHz, DMSO-$d_6$), δ (ppm): 164.7/ 167.6 (C9,C9'), 149.7/153.5 (C13,C13'), 148.2 (C3), 146.1 (C4 e C19), 141.1/142.8 (C7, C7'), 133.8 (C6), 133.1 (C15), 132.7 (C14), 121.2 (C1), 117.7 (C8), 116.3 (C2), 114.5 (C5), 110.8 (C20), 18.3 (C22), 40.5 (C17), 30.1 (C18), 29.6 (C16), 20.8 (C21). *m*/*z* (Rel. Int.): 327.17020.

**(*E*)-3-(3,4-dihydroxyphenyl)-*N*'-((*R*,*E*)-2-methyl-5-(prop-1-en-2-yl)cyclohex-2-en-1-ylidene)acrylohydrazide (PQM-291, 10c)**

**MW:** 326.40 g/mol. **Chemical Formula:** $C_{19}H_{22}N_2O_3$. **Physical appearance:** yellow solid. **Melting range**: 204-205ºC. **Purity (HPLC)**: 100%. **Yield:** 34%. **IR** (ATR, $\nu_{max}$, $cm^{-1}$): 3299 (ν OH), 3243 (ν NH), 2972 ($\nu_s$ $CH_2$ or $\nu_{as}$ $CH_3$), 1648 (ν C=O), 1616 (ν C=N), 1603 (δ NH), 1514 (ν C=$C_{ar}$), 1370 and 1120 (δ OH and =C-O), 979 (δ C=$CH_2$), 816 (δ RC=CH). **$^1$H NMR** (300 MHz, DMSO-$d_6$), δ (ppm): 10.46-10.41 (s, 1H, H12), 9.46 (s, 1H, H11), 9.23 (s, 1H, H10), 7.37 (dt, *J*= 16.2 Hz *J*= 29.7 Hz, 1H, H7), 7.02 (d, *J*= 13.2

 doi:10.20944/preprints202504.2053.v1



Hz, 1H, H5), 6.89-6.93 (m, 1H, H16), 6.74 (dd, *J*= 12.1 Hz and *J*= 16.41 Hz, 2H, H2; H8), 6.15 (s, 1H, H15), 4.80 (t, *J*= 7.2 Hz, 2H, H20), 2.93 (t, *J*= 13.2 Hz, 1H, H18), 2.21-2.36 (m, 2H, H17; H16), 2.03-2.14 (m, 2H, H18; H16), 1.91-1.83 (s, 3H, H22), 1.76 (s, 3H, H21); **$^{13}$C NMR** (75 MHz, DMSO-$d_6$), δ (ppm): 162.7/ 167.6 (C9,C9'), 149.7/153.5 (C13,C13'), 148.1 (C3), 146.1 (C4), 146.0 (C19), 141.0/142.8 (C7, C7'), 133.8 (C6), 133.0 (C15), 132.7 (C14), 121.2 (C1), 117.7 (C8), 116.3 (C2), 114.1 (C5), 110.8 (C20), 40.5 (C17), 30.1 (C18), 29.6 (C16), 21.0 (C21), 18.5 (C22). *m/z* (Rel. Int.): 327.17022.

**(*E*)-3-(4-hydroxyphenyl)-*N*'-((*R*,*E*)-2-methyl-5-(prop-1-en-2-yl)cyclohex-2-en-1-ylidene)acrylohydrazide (PQM-292, 11d)**

**MW:** 310.40 g/mol. **Chemical Formula:** $C_{19}H_{22}N_2O_2$. **Physical appearance:** pale yellow solid. **Melting range**: 189-190ºC. **Purity**: 100%. **Yield:** 21%. **IR** (ATR, $\nu_{max}$, cm$^{-1}$): 3299 (ν OH), 3066 ($\nu_{as}$ $CH_2$), 3014 ($\nu_s$ $CH_2$), 2953 and 2922 ($\nu_{as/s}$ $CH_3$), 1654 (ν C=O), 1622 (ν C=N), 1601 (δ NH), 1516 (ν C=$C_{ar}$), 1442 ($\delta_s$ $CH_2$), 1375 ($\delta_s$ $CH_3$), 1274 (ν C-N), 1200 (ν C-O), 1166 (δ OH + =C-O), 974 (δ HC=CH), 887 (δ =CH), 827 (δ $CH_{ar}$). **$^1$H NMR** (300 MHz, DMSO-$d_6$), δ (ppm): 10.4 (s, 1H, H10), 9.98 (s, 1H, H11), 7.31-7.59 (m, 3H, H1, H5; H7), 6.80 (t, *J* = 10.4 Hz, 3H, H2/H4; H8), 6.15 (s, 1H, H14), 4.80 (t, *J*= 7.65 Hz, 2H, H19), 2.93 (t, *J*= 13.4 Hz, 1H, H15), 2.32 (dd, *J*= 9.7 Hz, *J*= 15.9 Hz, 1H, H16), 2.02-2.22 (m, 3H, H17; H15), 1.85 (s,1H, H21), 1.75 (s, 1H, H20); **$^{13}$C NMR** (75 MHz, DMSO-$d_6$), δ (ppm): 167.6 (C9), 159.6 (C3), 153.5 (C12), 133.8 (C14), 133.0 (C13), 129.9 (C1, C5), 126.4 (C6), 117.8 (C8), 116.3 (C2, C4), 110.8 (C19), 40.6 (C16), 30.1 (C17), 29.6 (C15), 20.9 (C20), 18.5 (C21). *m/z* (Rel. Int.): 311.17534.

**(*E*)-3-(4-hydroxyphenyl)-*N*'-((*R*,*E*)-2-methyl-5-(prop-1-en-2-yl)cyclohex-2-en-1-ylidene)acrylohydrazide (PQM-293, 10d)**

**MW:** 310,40 g/mol. **Chemical Formula:** $C_{19}H_{22}N_2O_2$. **Physical appearance:** pale yellow solid. **Melting range**: 227-230ºC. **Purity (HPLC)**: 100%. **Yield:** 17%. **IR** ( ATR, $\nu_{max}$, cm$^{-1}$): 3301 (ν OH), 3067 ($\nu_{as}$ $CH_2$), 3014 e 2973 ($\nu_{s/as}$ $C_2$), 2953 and 2921 ($\nu_{as/s}$ $CH_3$), 1653 (ν C=O), 1622 (ν C=N), 1601 (δ NH), 1521 (ν C=$C_{ar}$), 1442 ($\delta_s$ $CH_2$), 1375 ($\delta_s$ $CH_3$), 1274 (ν C-N), 1201 (ν C-O), 1167 (δ OH + =C-O), 974 (δ HC=CH), 888 (δ =CH), 827 (δ $CH_{ar}$). **$^1$H NMR** (300 MHz, DMSO-$d_6$), δ (ppm): 10.4 (s, 1H, H10), 9.96 (s, 1H, H11), 7.31-7.58 (m, 3H, H1, H5; H7), 6.79 (t, *J*= 9.95 Hz, 3H, H2/H4; H8), 6.15 (s, 1H, H14), 4.80 (t, *J*= 8.05 Hz, 2H, H19), 2,93 (t, *J*= 14.3 Hz, 1H, H15), 2.28-2.36 (m, 1H, H16), 1.98-2.22 (m, 3H, H17; H15), 1.85 (s,1H, H21), 1.75 (s, 1H, H20); **$^{13}$C NMR** (75 MHz, DMSO-$d_6$), δ (ppm): 167.6 (C9), 159.6 (C3), 153.5 (C12), 133.8 (C14), 133.0 (C13), 130.0 (C1, C5), 126.4 (C6), 117.8 (C8), 116.3 (C2, C4), 110.8 (C19), 40.6 (C16), 30.1 (C17), 29.6 (C15), 20.9 (C20), 18.4 (C21). *m/z* (Rel. Int.): 311.17540.

**(*E*)-3-(4-methoxyphenyl)-*N*'-((*R*,*E*)-2-methyl-5-(prop-1-en-2-yl)cyclohex-2-en-1-ylidene)acrylohydrazide (PQM-294, 11e)**

**MW:** 324,42 g/mol. **Chemical Formula:** $C_{20}H_{24}N_2O_2$. **Physical appearance:** pale yellow solid. **Melting range**: 230-232ºC. **Purity (HPLC)**: 100%. **Yield:** 85%. **IR** ( ATR, $\nu_{max}$, cm$^{-1}$): 3161 (ν NH), 3073 ($\nu_{as}$ $CH_2$), 3031 ($\nu_s$ $CH_2$), 2968 and 2918 ($\nu_{as/s}$ $CH_3$), 2835 ($\nu_s$ $OCH_3$), 1657 (ν C=O), 1617 (ν C=N), 1595 (δ NH), 1509 (ν C=$C_{ar}$), 1463 ($\delta_s$ $CH_2$), 1374 ($\delta_s$ $CH_3$), 1252 ($\nu_{as}$ C-O), 1166 (ν C-N), 984 (δ HC=CH), 892 (δ =CH), 817 (δ $CH_{ar}$). **$^1$H NMR** (300 MHz, $CDCl_3$), δ (ppm): 1.80 (s, 3H, H20), 1.97 (S, 3H, H21), 2.07-2.17 (m, 2H, H17; H15), 2.28-2.48 (m, 2H, H16; H15), 2.89 (dd, *J*= 16.0.Hz, *J*= 3.5 Hz, 1H, H17), 3.84 (s, 3H, H10), 4.84 (s, 2H), 6.15 (d, *J*= 5.6 Hz, 1H, H14), 6.92 (d, *J*= 8.6 Hz, 2H, H2, H4), 7.48 (d, *J*= 16.0 Hz, 1H, H8), 7.54 (d, *J*= 8.6 Hz, 2H, H1; H5), 7.77 (d, *J*= 16.0 Hz, 1H, H7), 9.49 (s, 1H, H11). **$^{13}$CNMR** (75 MHz, $CDCl_3$), δ (ppm): 168.2 (C9), 161.1 (C3), 149.6 (C18), 147.5 (C7), 142.9 (C13), 132.8 (C14), 129.8 (C1, C5), 128.1 (C6), 114.4 (C8), 114.2 (C2, C4), 110.3 (C19), 55.6 (C10), 40.6 (C16), 30.1 (C17), 28.8 (C15), 20.8 (C20), 17.9 (C21). *m/z* (Rel. Int.): 325.19118.

**(*E*)-3-(4-methoxyphenyl)-*N*'-((*R*,*E*)-2-methyl-5-(prop-1-en-2-yl)cyclohex-2-en-1-ylidene)acrylohydrazide (PQM-295, 10e)**

**MW:** 324,42 g/mol**. Chemical Formula:** $C_{20}H_{24}N_2O_2$. **Physical appearance:** pale yellow solid. **Melting range**: 215-216ºC. **Purity (HPLC)**: 100%. **Yield:** 79%. **IR** (ATR, $\nu_{max}$, cm$^{-1}$): 3162 (ν NH), 3073 ($\nu_{as}$ $CH_2$), 3032 ($\nu_s$ $CH_2$), 2968 and 2918 ($\nu_{as/s}$ $CH_3$), 2835 ($\nu_s$ $OCH_3$), 1658 (ν C=O), 1617 (ν C=N), 1595 (δ NH), 1510 (ν C=$C_{ar}$), 1463 ($\delta_s$ $CH_2$), 1375 ($\delta_s$ $CH_3$), 1252 ($\nu_{as}$ C-O), 1166 (ν C-N), 984 (δ HC=CH), 893 (δ =CH), 817 (δ $CH_{ar}$). **$^1$H NMR** (300 MHz, $CDCl_3$), δ (ppm): 9.50 (s, 1H, H11), 7.77 (d, *J*= 16.0 Hz, 1H, H7), 7.54 (d, *J*= 8.6 Hz, 2H, H1; H5), 7.46 (d, *J*= 16.0 Hz, 1H, H8), 6.92 (d, *J*= 8.6 Hz, 2H, H2, H4), 6.15

 doi:10.20944/preprints202504.2053.v1



(d, *J*= 4.3 Hz, 1H, H14), 4.84 (s, 2H, H19), 3.84 (s, 3H, H10), 2.89 (dd, *J*= 16.1 Hz, *J*= 2.9 Hz, 1H, H17), 2.30-2.48 (m, 2H, H16; H15), 2.12 (dd, *J*= 14.4 Hz, *J*= 13.1 Hz, 2H, H17; H15), 1.98 (s, 3H, H21), 1.80 (s, 3H, H20); **$^{13}$C NMR** (75 MHz, $CDCl_3$), δ (ppm): 168.2 (C9), 161.1 (C3), 149.6 (C18), 147.5 (C7), 142.9 (C13), 132.8 (C14), 129.8 (C1, C5), 128.1 (C6), 114.4 (C8), 114.2 (C2, C4), 110.3 (C19), 55.4 (C10), 40.6 (C16), 30.1 (C17), 28.9 (C15), 20.8 (C20), 17.9 (C21). *m*/*z* (Rel. Int.): 325.19113.

**(*E*)-*N*'-((*S*,*E*)-2-methyl-5-(prop-1-en-2-yl)cyclohex-2-en-1-ylidene)-3-(4-(trifluoromethyl)phenyl)acrylohydrazide (PQM-300, 11f)**

**MW:** 362,40 g/mol. **Chemical Formula:** $C_{20}H_{21}F_3N_2O$. **Physical appearance:** white solid. **Melting range**: 220-221ºC. **Purity (HPLC)**: 100%. **Yield:** 70%. **IR** (ATR, $\nu_{max}$, $cm^{-1}$): 3168 (ν NH), 1688 (ν C=O), 1624 (δ NH), 1575 (ν C=N), 1318 and 1124 (ν $CF_3$), 979 (δ HC=CH), 895 (δ =CH), 831 (δ $CH_{ar}$). **$^1$H NMR** (300 MHz, $CDCl_3$), δ (ppm): 9.26 (s, 1H, H11), 7.81 (d, *J* = 16.1 Hz, 1H, H7), 7.62-7.70 (m, 5H, H1; H2; H4; H5; H8), 6.19 (d, *J*= 7.1 Hz, 1H, H14), 4,84 (d, *J*= 5.6 Hz 2H, H19), 2.83 (dd, *J*= 15.7 Hz, *J*= 4.0 Hz, 1H, H17), 2.30-2.48 (m, 2H, H16; H15), 2.07-2.18 (m, H17, H15), 1.97 (s, 3H, H21), 1.80 (s, 3H, H20); **$^{13}$C NMR** (75 MHz, $CDCl_3$), δ (ppm): 167.1 (C9), 150.2 (C3), 147.3 (C18), 141.4 (C7), 138.7 (C6), 133.5 (C14), 132.7 (C13), 128.3 (C1; C2; C4; C5), 119.4 (C8), 110.5 (C19), 40.6 (C16), 30.1 (C17), 28.8 (C15), 20.8 (C20), 17.9 (C21). *m*/*z* (Rel. Int.): 363.16785.

**(*E*)-*N*'-((*R*,*E*)-2-methyl-5-(prop-1-en-2-yl)cyclohex-2-en-1-ylidene)-3-(4-(trifluoromethyl)phenyl)acrylohydrazide (PQM-301, 10f)**

**MW:** 362,40 g/mol. **Chemical Formula:** $C_{20}H_{21}F_3N_2O$. **Physical appearance:** white solid. **Melting range**: 102-103ºC. **Purity (HPLC)**: 100%. **Yield:** 40%. **IR** (ATR, $\nu_{max}$, $cm^{-1}$): 3167 (ν NH), 2923 ($\nu_s$ $CH_2$), 1666 (ν C=O), 1623 (δ NH), 1575 (ν C=N), 1318 (ν C-$F_3$), 979 (δ HC=CH), 895 (δ =CH), 830 (δ $CH_{ar}$). **$^1$H NMR** (300 MHz, $CDCl_3$), δ (ppm): 9.36 (s, 1H, H11), 7.80 (d, *J*= 16.1 Hz, 1H, H7), 7.61-7.69 (m, 5H, H1; H2; H4; H5; H8), 6.18 (d, *J*= 7.1 Hz, 1H, H14), 4.83 (d, *J*= 4.8 Hz 2H, H19), 2.83 (dd, *J*= 15.9 Hz, *J*= 3,8 Hz, 1H, H17), 2.31-2.49 (m, 2H, H16; H15), 2.03-2.21 (m, H17, H15), 1.96 (s, 3H, H21), 1.79 (s, 3H, H20); **$^{13}$C NMR** (75 MHz, $CDCl_3$), δ (ppm): 167.2 (C9), 150.3 (C3), 147.3 (C18), 141.4 (C7), 138.7 (C6), 133.6 (C14), 132.7 (C13), 128.3 (C1; C2; C4; C5), 119.4 (C8), 110.4 (C19), 40.6 (C16), 30.1 (C17), 28.8 (C15), 20.8 (C20), 17.9 (C21). *m*/*z* (Rel. Int.): 363.16781.

**(*E*)-3-(2-hydroxyphenyl)-*N*'-((*R*,*E*)-2-methyl-5-(prop-1-en-2-yl)cyclohex-2-en-1-ylidene)acrylohydrazide (PQM-302, 11g)**

**MW:** 310,39 g/mol. **Chemical Formula:** $C_{19}H_{22}N_2O_2$. **Physical appearance:** yellow solid. **Melting range**: 215-217ºC. **Purity (HPLC)**: 100%. **Yield:** 69%. **IR** (ATR, $\nu_{max}$, $cm^{-1}$): 3208 (ν OH), 1644 (ν C=O), 1599 (δ NH), 1451 (δ $CH_3$), 1200 (ν C-OH), 989 (δ HC=CH), 888 (δ =CH), 754 (δ $CH_{ar}$). **$^1$H NMR** (300 MHz, DMSO-$d_6$), δ (ppm): 10.13-10.46 (s, 1H, H11; H11'), 7.82 (t, *J*= 16.9 Hz, 1H, H7), 7.47-7.66 (m, 1H, H8), 7.20 (t, *J*= 7.8 Hz, 1H, H3), 6.82-7.01 (m, 3H, H2; H4; H5), 6.16 (s, 1H, H14), 4.78-4.83 (m, 2H, H19), 2.94 (t, *J*= 12.5 Hz, 1H, H17), 2.21-2.36 (m, 2H, H16; H15), 2.03-2.11 (m, 2H, H17, H15), 1.89-1.84 (s, 3H, H21), 1.76 (s, 3H, H20). **$^{13}$C NMR** (75 MHz, DMSO-$d_6$), δ (ppm): 167.9 (C9), 157.2 (C5), 153.8 (C12), 149.7 (C7), 148.3 (C18), 138.7 (C6), 138.0 (C13), 136.2 (C3), 133.1 (C14), 133.9 (C1), 122.2 (C8), 121.7 (C6), 120.6 (C2), 117.7 (C6), 116.7 (C4), 110.8 (C19), 40.6 (C16), 30.2 (C17), 29.6 (C15), 21.0 (C20), 18.5 (C21). *m*/*z* (Rel. Int.): 311.17541.

**(*E*)-3-(2-hydroxyphenyl)-*N*'-((*R*,*E*)-2-methyl-5-(prop-1-en-2-yl)cyclohex-2-en-1-ylidene)acrylohydrazide (PQM-303, 10g)**

**MW:** 310,39 g/mol. **Chemical Formula:** $C_{19}H_{22}N_2O_2$. **Physical appearance:** pale yellow solid. **Melting range**: 231-233ºC. **Purity (HPLC)**: 100%. **Yield:** 60%. **IR** (ATR, $\nu_{max}$, $cm^{-1}$): 3208 (ν OH), 1644 (ν C=O), 1651 (ν C=N), 1599 (δ NH), 1451 (δ $CH_3$), 1200 (ν C-OH), 989 (δ HC=CH), 889 (δ =CH), 754 (δ $CH_{ar}$). **$^1$H NMR** (300 MHz, DMSO-$d_6$), δ (ppm): 10.41-10.52 (s, 1H, H10), 10.13 (s, 1H, H11), 7.81 (t, *J*= 17.1 Hz, 1H, H7), 7.56 (dd, *J*= 11.2 Hz and *J*= 44.2 Hz 1H, H8), 7,20 (t, *J* = 7.75.Hz, 1H, H3), 6.84-6.92 (m, 3H, H2; H4; H1), 6.16 (s, 1H, H14), 4.78-4.83 (m, 2H, H19), 2.94 (t, *J*= 13.6 Hz, 1H, H17), 2.29 (dd, *J*= 14.7 Hz e *J*= 26.2 Hz, 2H, H16; H15), 2.09 (dd, *J*= 15.5 Hz and *J*= 28.0 Hz, 2H, H17; H15), 1.88-1.84 (s, 3H, H21;H21'), 1.76 (s, 3H, H20); **$^{13}$C NMR** (75 MHz, DMSO-$d_6$), δ (ppm): 167.4 (C9), 156.4 (C5), 153.3 (C12), 149.2 (C7), 147.8 (C18), 138.7 (C6), 137.5 (C13), 135.7 (C3), 133.4 (C14), 132.6 (C1), 130.8 (C8),

 doi:10.20944/preprints202504.2053.v1



121.7 (C6), 119.4 (C2), 116.2 (C4), 110.3 (C19), 40.6 (C16), 29.7 (C15, C17), 20.5 (C20), 18.0 (C21). *m*/*z* (Rel. Int.): 311.17543.

**(*E*)-3-(benzo[*d*][1,3]dioxol-5-yl)-*N*'-((*S*,*E*)-2-methyl-5-(prop-1-en-2-yl)cyclohex-2-en-1-ylidene)acrylohydrazide (PQM-304, 11h)**

**MW:** 338,41 g/mol. **Chemical Formula:** $C_{20}H_{22}N_2O_3$. **Physical appearance:** pale yellow solid. **Melting range**: 244-245ºC. **Purity (HPLC)**: 100%. **Yield:** 70%. **IR** (ATR, ν max, cm-1): 3155 (ν NH), 2916 ($\nu_s$ $CH_2$), 1669 (ν C=O), 1629 (C=N), 1609 (δ NH), 1485 (δ $CH_2$), 1361 (δ $CH_3$), 1239 ($\nu_{ass}$ C-O-C), 1035 ($\nu_s$ C-O), 973 (δ HC=CH). **$^1$H NMR** (300 MHz, $CDCl_3$), δ (ppm): 9,31 (s, 1H, H11), 7,72 (d, *J* = 15,87Hz, 1H, H7), 7,40 (d, *J* = 15,90Hz, 1H, H8), 7,11 (s, 1H, H1), 7,06 (d, *J* = 8,80Hz, 1H, H5), 6,83 (d, *J* = 7,98Hz, 1H, H4), 6,15 (d, *J* = 5,98Hz, 1H, H14), 6,01 (s, 2H, H10), 4,83 (s, 2H, H19), 2,85 (dd, *J* = 3,74Hz e *J* = 15,89Hz 1H, H17), 2,37-2,48 (m, 1H, H16), 2,28-2,36 (m, 1H, H15), 2,10-2,18 (m, 2H, H17, H15), 1,97 (s, 3H, H21), 1,80 (s, 3H, H20); **$^{13}$C NMR** (75 MHz, $CDCl_3$), δ (ppm): 167,9 (C9), 149,6 (C3), 149,3 (C12), 148,2 (C2), 147,4 (C18), 143,0 (C7), 133,0 (C13), 132,9 (C6), 129,8 (C5), 124,5 (C8), 114,8 (C1), 110,4 (C4), 108,5 (C19), 106,6 (C14), 101,5 (C10), 40,6 (C16), 30,1(C17), 28,8 (C15), 20,8 (C20), 17,9 (C21). *m*/*z* (Rel. Int.): 339.17039.

**(*E*)-3-(benzo[*d*][1,3]dioxol-5-yl)-*N*'-((*R*,*E*)-2-methyl-5-(prop-1-en-2-yl)cyclohex-2-en-1-ylidene)acrylohydrazide (PQM-305, 10h)**

**MW:** 338,41 g/mol. **Chemical Formula:** $C_{20}H_{22}N_2O_3$. **Physical appearance:** pale yellow solid. **Melting range**: 237-239ºC. **Purity**: 100%. **Yield:** 17%. **IR** (ATR, ν max, cm-1): 3355 (ν NH), 1653 (ν C=O), 1610 (C=N), 1595 (δ NH), 1489 (δ $CH_2$), 1374 (δ $CH_3$), 1254 ($\nu_{ass}$ C-O-C), 1102 ($\nu_s$ C-O), 985 (δ HC=CH). **$^1$H NMR** (300 MHz, $CDCl_3$), δ (ppm): 9,08 (s, 1H, H11), 7,73 (d, *J* = 15,9Hz, 1H, H7), 7,39 (d, *J* = 15,95Hz, 1H, H8), 7,12 (s, 1H, H1), 7,06 (dd, *J* = 8,11Hz, *J* = 1,03Hz, 1H, H5), 6,83 (d, *J* = 7,98Hz, 1H, H4), 6,16 (d, *J* = 5,68Hz, 1H, H14), 6,02 (s, 2H, H10), 4,84 (d, *J* = 5,62Hz, 2H, H19), 2,80 (dd, *J* = 3,84Hz e *J* = 15,28Hz 1H, H17), 2,29-2,46 (m, 2H, H16 e H15), 2,12 (dd, *J*=6,24Hz e *J*=8,34Hz, *J*=15,54Hz 2H, H17, H15), 1,97 (s, 3H, H21), 1,79 (s, 3H, H20), **$^{13}$C NMR** (75 MHz, $CDCl_3$), δ (ppm): 167,8 (C9), 149,5 (C3), 149,3 (C12), 148,2 (C2), 147,4 (C18), 143,1 (C7), 133,0 (C13), 132,8 (C6), 129,8 (C5), 124,5 (C8), 114,7 (C1), 110,4 (C4), 108,6 (C19), 106,6 (C14), 101,5 (C10), 40,6 (C16), 30,1 (C17), 28,7 (C15), 20,8 (C20), 17,9 (C21). *m*/*z* (Rel. Int.): 339.17044.

**(*E*)-3-(4-chlorophenyl)-*N*'-((*S*,*E*)-2-methyl-5-(prop-1-en-2-yl)cyclohex-2-en-1-ylidene)acrylohydrazide (PQM-306, 11i)**

**MW:** 328,84 g/mol. **Chemical Formula:** $C_{19}H_{21}ClN_2O$. **Physical appearance:** white solid. **Melting range**: 215-216ºC. **Purity**: 100%. **Yield:** 63%. **IR** (ATR, ν max, cm-1): 3167 (ν NH), 2919 ($\nu_s$ $CH_2$), 1663 (ν C=O), 1617 (C=N), 1489 (δ $CH_2$), 1361 (δ $CH_3$), 1088 ($\nu_s$ C-Cl), 976 (δ HC=CH), 815 (δ $CH_{ar}$). **$^1$H NMR** (300 MHz, $CDCl_3$), δ (ppm): 8,97 (s, 1H, H10), 7,76 (d, *J* = 16,37Hz, 1H, H7), 7,50-7,56 (m, 3H, H2, H4, H8), 7,37 (d, *J* = 8,43, 2H, H1, H5), 6,18 (s, 1H, H13), 4,83 (d, *J* = 10,57Hz, 2H, H18), 2,78 (dd, *J* = 3,94Hz e *J* = 15,79Hz 1H, H16), 2,31-2,46 (m, 2H, H14, H15), 2,11 (dd, *J* = 13,93Hz e *J* = 25,80Hz, 2H, H16, H14), 1,97 (s, 3H, H20), 1,79 (s, 3H, H19); **$^{13}$C NMR** (75 MHz, $CDCl_3$), δ (ppm): 167,3 (C9), 149,7 (C11), 147,3 (C17), 141,9 (C7), 135,8 (C12), 133,8 (C13), 133,3 (C6), 132,7 (C3), 129,3 (C2 e C4), 129,1 (C1 e C5), 117,3 (C8), 110,5 (C18), 40,6 (C15), 30,1 (C16), 28,6 (C14), 20,8 (C19), 18,0 (C20). *m*/*z* (Rel. Int.): 329.14164.

**(*E*)-3-(4-chlorophenyl)-*N*'-((*R*,*E*)-2-methyl-5-(prop-1-en-2-yl)cyclohex-2-en-1-ylidene)acrylohydrazide (PQM-307, 10i)**

**MW:** 328,84 g/mol. **Chemical Formula:** $C_{19}H_{21}ClN_2O$. **Physical appearance:** pale yellow solid. **Melting range**: 234-236ºC. **Purity**: 100%. **Yield:** 71%. **IR** (ATR, ν max, cm-1): 3166 (ν NH), 2916 ($\nu_s$ $CH_2$), 1663 (ν C=O), 1617 (C=N), 1489 (δ $CH_2$), 1360 (δ $CH_3$), 1087 ($\nu_s$ C-Cl), 976 (δ HC=CH), 815 (δ $CH_{ar}$). **$^1$H NMR** (300 MHz, $CDCl_3$), δ (ppm): 8,92 (s, 1H, H10), 7,76 (d, *J* = 16,05Hz, 1H, H7), 7,51-7,55 (m, 3H, H2, H4, H8), 7,37 (d, *J* = 8,49Hz, 2H, H1, H5), 6,18 (d, *J* = 4,84Hz, 1H, H13), 4,82 (d, *J* = 11,28Hz, 2H, H18), 2,76 (dd, *J* = 3,86Hz e *J* = 15,90Hz 1H, H16), 2,29-2,49 (m, 2H, H14, H15), 2,13 (m, *J* = 7,47Hz, *J* = 10,063Hz e *J* = 28,31Hz, 2H, H16, H14), 1,97 (s, 3H, H20), 1,79 (s, 3H, H19), **$^{13}$C NMR** (75 MHz, $CDCl_3$), δ (ppm): 167,2 (C9), 149,7 (C11), 147,3 (C17), 141,9 (C7), 135,8 (C12), 133,8 (C13), 133,2 (C6),

 doi:10.20944/preprints202504.2053.v1



132,7 (C3), 129,3 (C2 e C4), 129,1 (C1 e C5), 117,3 (C8), 110,5 (C28), 40,6 (C15), 30,0 (C16), 28,6 (C14), 20,8 (C19), 17,9 (C20). *m/z* (Rel. Int.): 341.18622.

**(*E*)-3-(3-hydroxy-4-methoxyphenyl)-*N*'-((*R*,*E*)-2-methyl-5-(prop-1-en-2-yl)cyclohex-2-en-1-ylidene)acrylohydrazide (PQM-308, 11j)**

**MW:** 340,42 g/mol. **Chemical Formula:** $C_{20}H_{24}N_2O_3$. **Physical appearance:** yellow solid. **Melting range**: 190-192ºC. **Purity**: 100%. **Yield:** 30%. **IR** (ATR, v max, cm-1): 3362 (ν OH), 2911 ($\nu_s$ $CH_2$), 2835 ($\nu_s$ $CH_3$), 1647 (C=O), 1598 (δ NH), 1506 (δ C=$C_{ar}$), 1274 (ν C-O-C), 974 (δ CH), 795 (δ $CH_{ar}$). **$^1$H NMR** (300 MHz, $CDCl_3$), δ (ppm): 9,21 (s, 1H, H12), 7,72 (d, *J* = 16,0Hz, 1H, H7), 7,42 (d, *J* = 16,0Hz, 1H, H8), 7,23 (s, 1H, H5), 7,08 (d, *J* = 8,8Hz, 1H, H1), 6,86 (d, *J* = 8,2Hz, 1H, H2), 6,15 (d, *J* = 4,9Hz, 1H, H15), 5,85 (s, 1H, H10), 4,83 (d, *J* = 5,2Hz, 2H, H20), 3,93 (s, 3H, H11), 2,82 (dd, *J* = 2,5Hz, *J*=15,3Hz, 1H, H18), 2,44 (t, *J* = 11,7Hz 1H, H17), 2,32 (dd, *J* = 5,0Hz, *J* = 16,9Hz, 1H, H16), 2,11 (dd, *J* = 11,1Hz, *J* = 26,3Hz, 2H, H18, H16), 1,97 (s, 3H, H22), 1,79 (s, 3H, H21); **$^{13}$C** NMR (75 MHz, $CDCl_3$), δ (ppm): 168,0 (C9), 149,5 (C3), 148,3 (C4), 147,4 (C19), 145,8 (C14), 143,2 (C7), 132,9 (C15), 129,0 (C6), 122,2 (C1), 114,8 (C8), 113,0 (C5), 110,4 (C2), 110,5 (C20), 56,0 (C11), 40,6 (C17), 30,1 (C18), 28,7 (C16), 20,8 (C21), 17,9 (C22). *m/z* (Rel. Int.): 341.18600.

**(E)-3-(3-hydroxy-4-methoxyphenyl)-*N*'-((*R*,E)-2-methyl-5-(prop-1-en-2-yl)cyclohex-2-en-1-ylidene)acrylohydrazide (PQM-309, 10j)**

**MW:** 340,42 g/mol. **Chemical Formula:** $C_{20}H_{24}N_2O_3$. **Physical appearance:** yellow solid. **Melting range**: 194-195ºC. **Purity**: 100%. **Yield:** 24%. **IR** (ATR, v max, cm-1): 3243 (ν OH), 2911 ($\nu_s$ $CH_2$), 2836 ($\nu_s$ $CH_3$), 1647 (C=O), 1598 (δ NH), 1557 (ν C=N), 1506 (δ C=$C_{ar}$), 1274 (ν C-O-C), 975 (δ CH), 795 (δ $CH_{ar}$). **$^1$H NMR** (300 MHz, $CDCl_3$), δ (ppm): 9,03 (s, 1H, H12), 7,73 (d, *J* = 15,8Hz, 1H, H7), 7,41 (d, *J* = 16,0Hz, 1H, H8), 7,24 (d, *J* = 1,6Hz, 1H, H5), 7,08 (dd, *J* = 8,8Hz, *J* = 1,7Hz, 1H, H1), 6,86 (d, *J* = 8,3Hz, 1H, H2), 6,15 (d, *J* = 5,6Hz, 1H, H15), 5,78 (s, 1H, H10), 4,82 (d, *J* = 8,6Hz, 2H, H20), 3,93 (s, 3H, H11), 2,79 (dd, *J* = 3,6Hz, *J* = 16,1Hz, 1H, H18), 2,28-2,48 (m, 2H, H17 e H16), 2,12 (dd, *J* = 8,1Hz, *J* = 22,0Hz, 2H, H18, H16), 1,97 (s, 3H, H22), 1,79 (s, 3H, H21); **$^{13}$C NMR** (75 MHz, $CDCl_3$), δ (ppm): 167,9 (C9), 149,4 (C3), 148,3 (C4), 147,4 (C19), 145,7 (C14), 143,3 (C7), 132,9 (C15), 129,0 (C6), 122,2 (C1), 114,8 (C8), 112,9 (C5), 110,4 (C2), 110,5 (C20), 56,0 (C11), 40,6 (C17), 30,1 (C18), 28,6 (C16), 20,8 (C21), 17,9 (C22). *m/z* (Rel. Int.): 341.18580.

**(*E*)-3-(4-hydroxy-3,5-dimethoxyphenyl)-*N*'-((*S*,*E*)-2-methyl-5-(prop-1-en-2-yl)cyclohex-2-en-1-ylidene)acrylohydrazide (PQM-375, 10k)**

**MW:** 370,45 g/mol**. Chemical Formula:** $C_{21}H_{26}N_2O_4$. **Physical appearance:** pale yellow solid. **Melting range**: 217-219ºC. **Purity**: 100%. **Yield:** 51%. **IR** (ATR, v max, cm-1): 1652 (C=O), 1609 (δ NH), 1510 (ν C=N), 1456 (δ C=$C_{ar}$), 1322 (ν C-O-C), 981 (δ CH), 605 (δ $CH_{ar}$). **$^1$H NMR** (300 MHz, DMSO-$d_6$), δ (ppm): 10,34 (s, 1H, H13), 7,37-7,57 (m, 1H, H7), 6,69 (s, 2H, H1 e H5), 6,80 (d, *J* = 15,4Hz, 1H, H8), 6,15 (s, 1H, H16), 4,82 (d, *J* = 10,2 Hz, 2H, H21), 3,80 (s, 6H, H10 e H12), 2,91 (d, *J* = 14,5Hz, 1H, H19), 2,30 (dd, *J* = 14,9Hz, *J* = 32,1Hz, 2H, H18 e H17), 2,10 (dd, *J* = 13,2Hz, *J* = 26,3Hz, 2H, H19, H17), 1,84 (s, 3H, H22), 1,76 (s, 3H, H23); **$^{13}$C NMR** (75 MHz, DMSO-$d_6$), δ (ppm): 167,1 e 162,1 (C9), 153,1 (C14), 148,1 (C2, C4), 147,8 (C20), 140,9 (C7), 137,6 (C3), 133,4 (C15), 132,6 (C16), 125,3 (C8), 117,8 (C6), 110,4 (C21), 105,5 (C1, C5), 56,0 (C10, C12), 40,4 (C18), 29,6 (C19), 29,1 (C17), 20,5 (C22), 18,0 (C23). *m/z* (Rel. Int.): 371.19604.

**(E)-3-(4-hydroxy-3,5-dimethoxyphenyl)-*N*'-((*S*,E)-2-methyl-5-(prop-1-en-2-yl)cyclohex-2-en-1-ylidene)acrylohydrazide (PQM-376, 11k)**

**MW:** 370,45 g/mol. **Chemical Formula:** $C_{21}H_{26}N_2O_4$. **Physical appearance:** pale yellow solid. **Melting range**: 196-197ºC. **Purity**: 95%. **Yield:** 53%. **IR** (ATR, v max, cm-1): 1652 (C=O), 1612 (δ NH), 1512 (ν C=N), 1456 (δ C=$C_{ar}$), 1323 (ν C-O-C), 980 (δ CH), 604 (δ $CH_{ar}$). **$^1$H NMR** (300 MHz, C*D*$Cl_3$), δ (ppm): 8,85 (s, 1H, H13), 7,73 (d, *J* = 15,8 Hz, 1H, H7), 7,41 (d, *J* = 15,7 Hz, 1H, H8), 6,84 (s, 2H, H1 e H5), 6,16 (d, *J* = 7,1Hz 1H, H16), 5,81 (s, 1H, H11), 4,82 (d, *J* = 10,9 Hz, 2H, H21), 3,93 (s, 6H, H10 e H12), 2,76 (dd, *J* = 4,1Hz, *J* = 15,4Hz 1H, H19), 2,44 (dd, *J* = 8,4Hz, *J* = 19,8Hz, 1H, H18), 2,28-2,38 (m,1H, H17), 2,04-2,18 (m, 2H, H19, H17), 1,96 (s, 3H, H22), 1,79 (s, 3H, H23); **$^{13}$C NMR** (75 MHz, C*D*$Cl_3$), δ (ppm): 167,7 (C9), 149,3 (C12), 147,3 (C20), 147,2 (C2, C4), 143,7 (C7), 136,9 (C3), 133,1 (C16), 132,7

 doi:10.20944/preprints202504.2053.v1



(C15), 126,9 (C6), 114,7 (C8), 110,5 (C21), 105,2 (C1, C5), 56,3 (C10, C12), 40,6 (C18), 30,1 (C19), 28,6 (C17), 20,8 (C22), 17,7 (C23). *m/z* (Rel. Int.): 371.19626.

**(*E*)-3-(4-(dimethylamino)phenyl)-*N*'-((*R*,*E*)-2-methyl-5-(prop-1-en-2-yl)cyclohex-2-en-1-ylidene)acrylohydrazide (PQM-377, 10l)**

**MW:** 337,46 g/mol. **Chemical Formula:** $C_{21}H_{27}N_3O$. **Physical appearance:** pale yellow solid. **Melting range**: 236-237ºC. **Purity**: 72%. **Yield:** 53%. **IR** (ATR, v max, cm-1): 3155 e 2914 (δ NH), 1651 (C=O), 1591 (δ NH), 1553 (ν C=N), 1350 (δ C=$C_{ar}$), 1227 (ν C-O-C), 937 (δ CH), 645 (δ $CH_{ar}$). **$^1$H NMR** (300 MHz, C*D*$Cl_3$), δ (ppm): 9,01 (s, 1H, H12), 7,76 (d, *J* = 15,8 Hz, 1H, H7), 7,49 (d, *J* = 8,6Hz, 2H, H1 e H5), 7,35 (d, *J* = 15,9 Hz, 1H, H8), 6,69 (d, *J* = 8,6 Hz, 2H, H2 e H4), 6,13 (d, *J* = 5,7 Hz 1H, H15), 4,82 (d, *J* = 6,4 Hz, 2H, H20), 3,0 (s, 6H, H10 e H11), 2,81 (dd, *J* = 3,9 Hz, *J* = 15,6Hz 1H, H18), 2,43 (dd, *J* = 7,8Hz, *J* = 19,8Hz, 1H, H17), 2,31 (dt, *J* = 4,9 Hz, *J* = 10,3Hz,1H, H16), 2,03-2,17 (m, 2H, H18, H16), 1,97 (s, 3H, H21), 1,79 (s, 3H, H22), **$^{13}$C NMR** (75 MHz, C*D*$Cl_3$), δ (ppm): 168,5 (C9), 151,6 (C3), 148,8 (C13), 147,5 (C19), 143,9 (C7), 133,0 (C14), 132,5 (C15), 129,8 (C1 e C5), 123,3 (C6), 111,9 (C2 e C4), 111,3 (C8), 110,3 (C20), 40,7 (C17), 40,2 (C10 e C11), 30,1 (C18), 28,7 (C16), 20,8 (C22), 17,9 (C21). *m/z* (Rel. Int.): 338.22232.

**(*E*)-3-(4-(dimethylamino)phenyl)-*N*'-((*S*,*E*)-2-methyl-5-(prop-1-en-2-yl)cyclohex-2-en-1-ylidene)acrylohydrazide (PQM-378, 11l)**

**MW:** 337,46 g/mol. **Chemical Formula:** $C_{21}H_{27}N_3O$. **Physical appearance:** pale yellow solid. **Melting range**: 220-223ºC. **Purity**: 75%. **Yield:** 22%. **IR** (ATR, v max, cm-1): 3154 e 2914 (δ NH), 1651 (C=O), 1590 (δ NH), 1552 (ν C=N), 1360 (δ C=$C_{ar}$), 1227 (ν C-O-C), 987 (δ CH), 645 (δ $CH_{ar}$). **$^1$H NMR** (300 MHz, C*D*$Cl_3$), δ (ppm): 9,07 (s, 1H, H12), 7,76 (d, *J* = 15,9 Hz, 1H, H7), 7,49 (d, *J* = 8,6 Hz, 2H, H1 e H5), 7,35 (d, *J* = 15,9 Hz, 1H, H8), 6,69 (d, *J* = 8,6 Hz, 2H, H2 e H4), 6,13 (d, *J* = 6,1 Hz 1H, H15), 4,82 (d, *J* = 5,3 Hz, 2H, H20), 3,01 (s, 6H, H10 e H11), 2,82 (dd, *J* = 4,0 Hz, *J* = 15,7 Hz 1H, H18), 2,44 (dt, *J* = 4,4Hz, *J* = 12,5Hz, 1H, H17), 2,31 (dt, *J* = 5,50 Hz, *J* = 11,4Hz, 1H, H16), 2,04-2,17 (m, 2H, H18, H16), 1,97 (s, 3H, H21), 1,79 (s, 3H, H22); **$^{13}$C NMR** (75 MHz, C*D*$Cl_3$), δ (ppm): 168,5 (C9), 151,6 (C3), 148,8 (C13), 147,5 (C19), 143,9 (C7), 133,0 (C14), 132,5 (C15), 129,8 (C1 e C5), 123,3 (C6), 111,9 (C2 e C4), 111,3 (C8), 110,3 (C20), 40,7 (C17), 40,2 (C10 e C11), 30,1 (C18), 28,7 (C16), 20,8 (C22), 17,9 (C21). *m/z* (Rel. Int.): 338.22235.

***N*'-((*R*,*E*)-2-methyl-5-(prop-1-en-2-yl)cyclohex-2-en-1-ylidene)cinnamohydrazide (PQM-379, 10m)**

**MW:** 294,39 g/mol. **Chemical Formula:** $C_{19}H_{22}N_2O$. **Physical appearance:** pale yellow solid. **Melting range**: 210-211ºC. **Purity**: 100%. **Yield:** 41%. **IR** (ATR, v max, cm-1): 3168, 3025 e 2916 (δ NH), 1660 (C=O), 1447 (ν C=N), 1358 (δ C=$C_{ar}$), 1218 (ν C-O-C), 886 (δ CH), 760 (δ $CH_{ar}$). **$^1$H NMR** (300 MHz, C*D*$Cl_3$), δ (ppm): 9,32 (s, 1H, H10), 7,81 (d, *J* = 16,0 Hz, 1H, H7), 7,55-7,60 (m, 3H, H1, H5, H3), 7,40 (d, *J* = 6,2 Hz, 3H, H2, H4, H8), 6,16 (d, *J* = 5,5 Hz 1H, H13), 4,83 (s, 2H, H19), 2,86 (dd, *J* = 4,0 Hz, *J* = 15,8 Hz 1H, H16), 2,40-2,50 (m, 1H, H15) , 2,28-2,37 (m, 1H, H14), 2,06-2,18 (m, 2H, H16, H14), 1,97 (s, 3H, H18), 1,80 (s, 3H, H20); **$^{13}$C NMR** (75 MHz, C*D*$Cl_3$), δ (ppm): 167,8 (C9), 149,7 (C11), 147,4 (C17), 143,3 (C7), 135,4 (C6), 133,1 (C13), 132,8 (C12), 129,9 (C3), 128,8 (C2, C4), 128,2 (C1 e C5), 116,9 (C8), 110,4 (C19), 40,6 (C15), 30,1 (C16), 28,8 (C14), 20,8 (C20), 17,9 (C18). *m/z* (Rel. Int.): 295.18033.

***N*'-((*S*,*E*)-2-methyl-5-(prop-1-en-2-yl)cyclohex-2-en-1-ylidene)cinnamohydrazide (PQM308, 11m)**

**MW:** 294,39 g/mol. **Chemical Formula:** $C_{19}H_{22}N_2O$. **Physical appearance:** pale yellow solid. **Melting range**: 185-186ºC. **Purity**: 100%. **Yield:** 34%. **IR** (ATR, v max, cm-1): 3171, 3057 e 2916 (δ NH), 1663 (C=O), 1447 (ν C=N), 1359 (δ C=$C_{ar}$), 1220 (ν C-O-C), 886 (δ CH), 760 (δ $CH_{ar}$). **$^1$H NMR** (300 MHz, C*D*$Cl_3$), δ (ppm): 9,28 (s, 1H, H10), 7,81 (d, *J* = 16,0 Hz, 1H, H7), 7,55-7,60 (m, 3H, H1, H5, H3), 7,40 (d, *J* = 6,1 Hz, 3H, H2, H4, H8), 6,16 (d, *J* = 5,8 Hz 1H, H13), 4,84 (d, *J* = 3,7 Hz, 2H, H19), 2,85 (dd, *J* = 3,9 Hz, *J* = 15,8 Hz 1H, H16), 2,40-2,51 (m, 1H, H14); **$^{13}$C NMR** (75 MHz, C*D*$Cl_3$), δ (ppm): 167,7 (C9), 149,7 (C11), 147,4 (C17), 143,3 (C7), 35,4 (C6), 133,1 (C13, C12), 129,9 (C3), 128,8 (C2, C4), 128,2 (C1 e C5), 116,9 (C8), 110,4 (C19), 40,6 (C15), 30,1 (C16), 28,8 (C14), 20,8 (C20), 17,9 (C18). *m/z* (Rel. Int.): 295.18027.

 doi:10.20944/preprints202504.2053.v1



*4.2. Molecular Docking*

For this study we evaluated the cannabinoid receptors CB1 and CB2, and TRPV1, which may be involved in the anti-inflammatory and antinociceptive activities in vivo (Table 2). The cannabinoid receptors were aligned with the super command from PyMOL™ Molecular Graphics System (version 2.5.0, Schrödinger, LLC, New York, NY), for this we used the CB1 (PDB ID 8GHV) structure. Protein preparation was carried out with the Protein Preparation Wizard of Maestro 13.9.135 (Schrödinger, LLC, New York, NY) with the protonation and tautomeric states predicted with PROPKA3 at neutral pH. The reference ligands and evaluated compounds (named PQM) were prepared with the LigPrep and Epik tools of Maestro, which helps to predict protonation states at neutral pH [36]. Docking studies were performed with the DockThor-VS platform (freely available at www.dockthor.lncc.br) using the Standard configuration of the search algorithm and a grid size of 22 Å in each dimension [37,38]. The docking protocol adopted in this work was validated by redocking the co-crystallized compounds, with the top-energy pose of all protein-ligand complexes being successfully predicted with RMSD values lower than 2 Å.

**Table 2.** Selected structures of cannabinoid receptors CB1 and CB2, and TRPV1 receptor, as well as the search space configuration used in the docking studies.

| Receptor | PDB / Resolution | Grid center | Cofactor / Water |
|---|---|---|---|
| CB1 | 8GHV / 2.8 Å | X=146.41, Y=143.88, Z=192.33 | None |
| | 5U09 / 2.6 Å | X=144.21 Y=148.71 Z=191.95 | 1 water molecule |
| CB2 | 5ZTY / 2.8 Å | X=147.27 Y=144.43 Z=190.03 | 1 water molecule |
| | 8GUR / 2.8 Å | X=148.56 Y=144.29 Z=190.45 | None |
| TRPV1 | 8GFA / 2.29 Å | X=105.36, Y=80.97, Z=88.36 | POV (cofactor), 1 water molecule |

*4.3. Animals*

Swiss Webster mice (25–30 g) were kindly donated by the Instituto Vital Brazil (Niterói, Rio de Janeiro, Brazil). Mice were maintained in the Animal Experimentation Department of the Institute of Biomedical Sciences in a room with a light-dark cycle of 12 h, 22 ± 2 °C to 60% to 80% humidity, and with food and water *ad libitum*. Animals were used only once throughout the experiments. All protocols were conducted in accordance with the principles and guidelines adopted by the National Council for the Control of Animal Experimentation (CONCEA), approved by the Ethical Committee for Animal Research (protocols numbers 31/19, 34/19, 28/20). All experimental protocols were performed during the light phase. Animal numbers per group were kept at a minimum, and at the end of each experiment, mice were killed by a ketamine/xylazine overdose.

*4.4. Drugs and Reagents*

Acetylsalicylic acid (ASA) was purchased from Sigma-Aldrich (St. Louis, MO, USA). Ethanol and formalin were purchased from Merck Inc. (Rio de Janeiro, Brazil). Morphine sulfate was kindly provided by Cristália (São Paulo, Brazil). Drugs were dissolved in saline (NaCl 0.9%) prior to use. All drugs were diluted just before their use.

*4.5. Administration of Compounds and Drugs*

All compounds were dissolved in saline to prepare 100 µmol/mL stock solutions. Before their use, solutions were freshly prepared from each stock solution using saline. Doses of 10 µmol/kg (final volume of 0.1 mL per animal) were administered by oral gavage. Acetylsalicylic acid (ASA, 1.100 µmol/kg) and morphine (5 µmol/kg) were used as reference drugs. The dose of ASA and morphine was chosen based on previous results obtained by our group when their $DE_{50}$ (*i.e.* the dose that caused a 50% reduction in the nociceptive or anti-inflammatory effect) was calculated. The control group was given vehicle only.

 doi:10.20944/preprints202504.2053.v1



*4.6. In Vivo Toxicity Test*

Mice received an oral administration of 100 μmol/kg of each compound. After 24 h, animals were euthanized with ketamine (50 mg/kg)/xylazine (20 mg/kg). A sample of blood was collected in a heparinized tube. The femur was removed, the ends were cut, and the bone marrow from each femur was washed with 1 mL of saline with heparin and collected. Samples of blood and bone marrow were submitted to a complete blood hemogram and cell count, respectively, in an automatic cell counter (PocH-100iV Diff, Sysmex, Kobe, Japan).

*4.7. Formalin-Induced Nociception*

This assay was performed as described by Sakurada and cols. and adapted by Matheus *et al*. [39,40] This model is characterized by a response that occurred in two phases. The first phase (acute neurogenic pain) occurred during the first 5 min after the intraplantar injection of formalin, and the second phase (inflammatory pain) occurred during the 15 to 30 min post-injection. Animals (n= 7, per group) received 20 μL of formalin (2.5% v/v) into the dorsal surface of the left hind paw. The time that the animal spent licking the injected paw was immediately recorded. Mice were pretreated with oral doses of 5a-5h, morphine, ASA, or vehicle, 60 min before the administration of formalin.

*4.8. Thermal-Induced Nociception (Hot Plate Test)*

Mice were tested, according to the method described by Sahley and Berntson and adapted by Matheus et al. [40,41]. Mice (n= 8 per group) were placed on a hot plate (Insight Equipment, São Paulo, Brazil) set at 55±1 °C. The reaction time (licking of paws or jumping) was recorded every 30 min post oral administration of compounds, vehicle, morphine or cannabidiol (CBD) until 180 min. The average reaction time (in seconds) obtained at 60 and 30 min before oral administration was considered to be baseline (normal reaction to the temperature). The area under the curve (AUC) graphs were calculated from time course graphs. The following formula, which is based on the trapezoid rule, was used to calculate the AUC: AUC= 30 × IB ((min 30) + (min 60) + (min 180)/2), where IB is the increase from the baseline (in %).

*4.9. Statistical Analysis*

The number of animals per group was indicated in each experiment. The results are presented as mean ± SD calculated using Prism Software 10.1.2 (GraphPad Software, La Jolla, CA, USA). One-way or two-way analysis of variance (ANOVA) followed by Tukey's post hoc test was used for unpaired data when more than two groups were compared to the same control. The post hoc tests were run only if F achieved the necessary level of statistical significance. When $p < 0.05$, group differences were considered significant.

## 5. Conclusions

Twenty-six CBD-based terpenyl-cinnamoyl-acyl-hydrazone analogues were successfully obtained, with overall yields of up to 64%. The antinociceptive effect of these compounds were investigated by the classical methods of the formalin and hot plate assay, which also assisted in the search for the mechanism of action.

In the formalin test 6 compounds showed comparable results to morphine in the 1$^{st}$ phase (neurogenic phase), especially PQM292 and PQM-293, while in the 2$^{nd}$ phase (inflammatory phase) PQM-292 showed a better result than morphine for chronic and inflammatory pain, which suggests a possible anti-inflammatory activity of this compound. In the hot plate assay, six compounds exhibited better results than morphine, especially PQM-274. These findings led to the investigation of the possible mechanism involved in the observed activities. In the computational studies, all compounds showed low affinity for the CB receptors, although this does not impact their antinociceptive activity. Regarding the TRPV1 channels, neither of the compounds interacted with the structural residues of this receptor, which can suggest that these CBD-based analogs can act

 doi:10.20944/preprints202504.2053.v1



through a different mechanism, such as TRPA1 or that they could be active after metabolization. Moreover, the position and nature of the substituents on the aromatic moiety of the structure of compounds seemed to have a significant impact in the observed results, suggesting that electronegative and small H-bond donor/acceptor substituents, such as hydroxy and methoxy groups, potentially favor acute and chronic antinociceptive activity, with possible anti-inflammatory properties.

**Supplementary Materials:** The following supporting information can be downloaded at the website of this paper posted on Preprints.org. Analytical and spectroscopic data available in the Supplementary Material.

**Author Contributions:** Conceptualization, M.L.S., J.P.B.P., C.V.J., P.D.F., V.S.G.; methodology, M.L.S., J.P.B. P., C.V.J., P.D.F., V.S.G., G.R.R.F.; data curation, M.L.S., J.P.B.P., G.R.R.F., M.A.A., H.M.R.S., A.C.P.L., E.A.O., T.B.S.G.; molecular docking, M.L.S., I.A.G., L.E.D.; writing, M.L.S., J.P.B.P., C.V.J., P.D.F., V.S.G.; supervision, C.V.J., P.D.F., V.S.G., I.A.G. All authors have read and agreed to the submitted version of the manuscript.

**Funding:** This research was supported by the National Council for Scientific and Technological Development (CNPQ, Brazil, #406739-2018-8, # 308557/2021-2; #306900/2023-8), Minas Gerais State Research Support Foundation (FAPEMIG, Brazil, #APQ-CEX00518-17), Fundação Carlos Chagas Filho de Apoio à Pesquisa (FAPERJ, Brazil # SEI-260003/003464/2022; SEI-260003/001154/2023), and INCT-INOFAR (Brazil, #465249/2014-0, #402176/2024-3).

**Institutional Review Board Statement:** All protocols were conducted in accordance with the principles and guidelines adopted by the National Council for the Control of Animal Experimentation (CONCEA), approved by the Ethical Committee for Animal Research (protocols numbers 31/19, 34/19, 28/20).

**Data Availability Statement:** The original contributions presented in this study are included in the article/supplementary material. Further inquiries can be directed to the corresponding author(s).

**Acknowledgments:** The authors are grateful to the Brazilian Agencies for fellowships to C.V.J., P.D.F., and L.E.D. (CNPq); P.D.F., I.A.G., L.E.D. (FAPERJ), and to M.L.S., J.P.B.P., G.R.R.F (CAPES, code number 001).

**Conflicts of Interest:** The authors declare no conflicts of interest.

## Abbreviations

The following abbreviations are used in this manuscript:

| | |
|---|---|
| CDB | Cannabidiol |
| CB1 | Cannabinoid receptor type 1 |
| CB2 | Cannabinoid receptor type 2 |
| TRPA1 | Transient receptor potential ankyrin 1 |
| TRPV1 | Transient receptor potential cation channel subfamily V member 1 |
| ASA | Acetylsalicylic acid |

### References

1. Jha, S.K.; Nelson, V.K.; Suryadevara, P.R.; Panda, S.P.; Pullaiah, C.P.; Nuli, M.V.; Kamal, M.; Imran, M.; Ausali, S.; Abomughaid, M.M.; et al. Cannabidiol and Neurodegeneration: From Molecular Mechanisms to Clinical Benefits. *Ageing Res Rev* **2024**, *100*, 102386, doi:10.1016/j.arr.2024.102386.
2. Silva-Cardoso, G.K.; Leite-Panissi, C.R.A. Chronic Pain and Cannabidiol in Animal Models: Behavioral Pharmacology and Future Perspectives. *Cannabis Cannabinoid Res* **2023**, *8*, 241–253, doi:10.1089/can.2022.0096.
3. Sideris, A.; Doan, L. V. An Overview of Cannabidiol. *Anesth Analg* **2024**, *138*, 54–68, doi:10.1213/ANE.0000000000006584.
4. Nazir, M.; Saleem, M.; Tousif, M.I.; Anwar, M.A.; Surup, F.; Ali, I.; Wang, D.; Mamadalieva, N.Z.; Alshammari, E.; Ashour, M.L.; et al. Meroterpenoids: A Comprehensive Update Insight on Structural Diversity and Biology. *Biomolecules* **2021**, *11*, 957, doi:10.3390/biom11070957.
5. Atakan, Z. Cannabis, a Complex Plant: Different Compounds and Different Effects on Individuals. *Ther Adv Psychopharmacol* **2012**, *2*, 241–254, doi:10.1177/2045125312457586.

 doi:10.20944/preprints202504.2053.v1




6. Pellati, F.; Borgonetti, V.; Brighenti, V.; Biagi, M.; Benvenuti, S.; Corsi, L. Cannabis Sativa L. and Nonpsychoactive Cannabinoids: Their Chemistry and Role against Oxidative Stress, Inflammation, and Cancer. *Biomed Res Int* **2018**, *2018*, 1–15, doi:10.1155/2018/1691428.
7. Martinez Naya, N.; Kelly, J.; Corna, G.; Golino, M.; Polizio, A.H.; Abbate, A.; Toldo, S.; Mezzaroma, E. An Overview of Cannabidiol as a Multifunctional Drug: Pharmacokinetics and Cellular Effects. *Molecules* **2024**, *29*, 473, doi:10.3390/molecules29020473.
8. Morales, P.; Reggio, P.H.; Jagerovic, N. An Overview on Medicinal Chemistry of Synthetic and Natural Derivatives of Cannabidiol. *Front Pharmacol* **2017**, *8*, 1–18, doi:10.3389/fphar.2017.00422.
9. Gong, X.; Sun, C.; Abame, M.A.; Shi, W.; Xie, Y.; Xu, W.; Zhu, F.; Zhang, Y.; Shen, J.; Aisa, H.A. Synthesis of CBD and Its Derivatives Bearing Various C4′-Side Chains with a Late-Stage Diversification Method. *J Org Chem* **2020**, *85*, 2704–2715, doi:10.1021/acs.joc.9b02880.
10. Zi, C.-T.; Xie, Y.-R.; Niu, Y.; Liu, Z.-H.; Yang, L.; Xi, Y.-K.; Li, Z.-J.; Zhang, F.-M.; Xiang, Z.-M.; Sheng, J. New Cannabidiol (CBD) Derivatives: Synthesis, Anti-Inflammatory Activity, and Molecular Docking. *Phytochem Lett* **2022**, *51*, 97–103, doi:10.1016/j.phytol.2022.08.004.
11. Morales, P.; Reggio, P.H.; Jagerovic, N. An Overview on Medicinal Chemistry of Synthetic and Natural Derivatives of Cannabidiol. *Front Pharmacol* **2017**, *8*, 1–18, doi:10.3389/fphar.2017.00422.
12. Atakan, Z. Cannabis, a Complex Plant: Different Compounds and Different Effects on Individuals. *Ther Adv Psychopharmacol* **2012**, *2*, 241–254, doi:10.1177/2045125312457586.
13. Hong, G.; Sideris, A.; Waldman, S.; Stauffer, J.; Wu, C.L. Legal and Regulatory Aspects of Medical Cannabis in the United States. *Anesth Analg* **2024**, *138*, 31–41, doi:10.1213/ANE.0000000000006301.
14. Vlad, I.M.; Nuță, D.C.; Căproiu, M.T.; Dumitrașcu, F.; Kapronczai, E.; Mük, G.R.; Avram, S.; Niculescu, A.G.; Zarafu, I.; Ciorobescu, V.A.; et al. Synthesis and Characterization of New N-Acyl Hydrazone Derivatives of Carprofen as Potential Tuberculostatic Agents. *Antibiotics* **2024**, *13*, 212, doi:10.3390/antibiotics13030212.
15. Belyaeva, E.R.; Myasoedova, Yu. V.; Ishmuratova, N.M.; Ishmuratov, G.Yu. Synthesis and Biological Activity of N-Acylhydrazones. *Russ J Bioorg Chem* **2022**, *48*, 1123–1150, doi:10.1134/S1068162022060085.
16. da Costa Salomé, D.; de Freitas, R.H.C.N.; Fraga, C.A.M.; Fernandes, P.D. Novel Regioisomeric Analogues of Naphthyl-N-Acylhydrazone Derivatives and Their Anti-Inflammatory Effects. *Int J Mol Sci* **2022**, *23*, 13562, doi:10.3390/ijms232113562.
17. Thota, S.; Rodrigues, D.A.; Pinheiro, P. de S.M.; Lima, L.M.; Fraga, C.A.M.; Barreiro, E.J. N-Acylhydrazones as Drugs. *Bioorg Med Chem Lett* **2018**, *28*, 2797–2806, doi:10.1016/j.bmcl.2018.07.015.
18. Fraga, C.; Barreiro, E. Medicinal Chemistry of N-Acylhydrazones: New Lead-Compounds of Analgesic, Antiinflammatory and Antithrombotic Drugs. *Curr Med Chem* **2006**, *13*, 167–198, doi:10.2174/092986706775197881.
19. Fraga, C.; Barreiro, E. Medicinal Chemistry of N-Acylhydrazones: New Lead-Compounds of Analgesic, Antiinflammatory and Antithrombotic Drugs. *Curr Med Chem* **2006**, *13*, 167–198, doi:10.2174/092986706775197881.
20. Duarte, C.; Barreiro, E.; Fraga, C. Privileged Structures: A Useful Concept for the Rational Design of New Lead Drug Candidates. *Mini-Reviews in Medicinal Chemistry* **2007**, *7*, 1108–1119, doi:10.2174/138955707782331722.
21. S.R. Murty, M.; R. Ram, K.; Venkateswara Rao, R.; S. Yadav, J.; Venkateswara Rao, J.; R. Velatooru, L. Synthesis of New S-Alkylated-3-Mercapto-1,2,4-Triazole Derivatives Bearing Cyclic Amine Moiety as Potent Anticancer Agents. *Lett Drug Des Discov* **2012**, *9*, 276–281, doi:10.2174/157018012799129882.
22. Hunskaar, S.; Hole, K. The Formalin Test in Mice: Dissociation between Inflammatory and Non-Inflammatory Pain. *Pain* **1987**, *30*, 103–114, doi:10.1016/0304-3959(87)90088-1.
23. Chichorro, J.G.; Lorenzetti, B.B.; Zampronio, A.R. Involvement of Bradykinin, Cytokines, Sympathetic Amines and Prostaglandins in Formalin-induced Orofacial Nociception in Rats. *Br J Pharmacol* **2004**, *141*, 1175–1184, doi:10.1038/sj.bjp.0705724.
24. Shields, S.D.; Cavanaugh, D.J.; Lee, H.; Anderson, D.J.; Basbaum, A.I. Pain Behavior in the Formalin Test Persists after Ablation of the Great Majority of C-Fiber Nociceptors. *Pain* **2010**, *151*, 422–429, doi:10.1016/j.pain.2010.08.001.

25. Parada, C.A.; Tambeli, C.H.; Cunha, F.Q.; Ferreira, S.H. The Major Role of Peripheral Release of Histamine and 5-Hydroxytryptamine in Formalin-Induced Nociception. *Neuroscience* **2001**, *102*, 937–944, doi:10.1016/S0306-4522(00)00523-6.
26. Matsumoto, K.; Horie, S.; Ishikawa, H.; Takayama, H.; Aimi, N.; Ponglux, D.; Watanabe, K. Antinociceptive Effect of 7-Hydroxymitragynine in Mice: Discovery of an Orally Active Opioid Analgesic from the Thai Medicinal Herb Mitragyna Speciosa. *Life Sci* **2004**, *74*, 2143–2155, doi:10.1016/j.lfs.2003.09.054.
27. Liu, Y.; Ji, L.; Eno, M.; Kudalkar, S.; Li, A.-L.; Schimpgen, M.; Benchama, O.; Morales, P.; Xu, S.; Hurst, D.; et al. ( R )- N -(1-Methyl-2-Hydroxyethyl)-13-( S )-Methyl-Arachidonamide (AMG315): A Novel Chiral Potent Endocannabinoid Ligand with Stability to Metabolizing Enzymes. *J Med Chem* **2018**, *61*, 8639–8657, doi:10.1021/acs.jmedchem.8b00611.
28. Gao, Y.; Cao, E.; Julius, D.; Cheng, Y. TRPV1 Structures in Nanodiscs Reveal Mechanisms of Ligand and Lipid Action. *Nature* **2016**, *534*, 347–351, doi:10.1038/nature17964.
29. De Gregorio, D.; McLaughlin, R.J.; Posa, L.; Ochoa-Sanchez, R.; Enns, J.; Lopez-Canul, M.; Aboud, M.; Maione, S.; Comai, S.; Gobbi, G. Cannabidiol Modulates Serotonergic Transmission and Reverses Both Allodynia and Anxiety-like Behavior in a Model of Neuropathic Pain. *Pain* **2019**, *160*, 136–150, doi:10.1097/j.pain.0000000000001386.
30. Comelli, F.; Giagnoni, G.; Bettoni, I.; Colleoni, M.; Costa, B. Antihyperalgesic Effect of a Cannabis Sativa Extract in a Rat Model of Neuropathic Pain: Mechanisms Involved. *Phytotherapy Research* **2008**, *22*, 1017–1024, doi:10.1002/ptr.2401.
31. Mitchell, V.A.; Harley, J.; Casey, S.L.; Vaughan, A.C.; Winters, B.L.; Vaughan, C.W. Oral Efficacy of Δ(9)-Tetrahydrocannabinol and Cannabidiol in a Mouse Neuropathic Pain Model. *Neuropharmacology* **2021**, *189*, 108529, doi:10.1016/j.neuropharm.2021.108529.
32. Britch, S.C.; Goodman, A.G.; Wiley, J.L.; Pondelick, A.M.; Craft, R.M. Antinociceptive and Immune Effects of Delta-9-Tetrahydrocannabinol or Cannabidiol in Male Versus Female Rats with Persistent Inflammatory Pain. *J Pharmacol Exp Ther* **2020**, *373*, 416–428, doi:10.1124/jpet.119.263319.
33. Arantes, A.L.F.; Carvalho, M.C.; Brandão, M.L.; Prado, W.A.; Crippa, J.A. de S.; Lovick, T.A.; Genaro, K. Antinociceptive Action of Cannabidiol on Thermal Sensitivity and Post-Operative Pain in Male and Female Rats. *Behavioural Brain Research* **2024**, *459*, 114793, doi:10.1016/j.bbr.2023.114793.
34. McNamara, C.R.; Mandel-Brehm, J.; Bautista, D.M.; Siemens, J.; Deranian, K.L.; Zhao, M.; Hayward, N.J.; Chong, J.A.; Julius, D.; Moran, M.M.; et al. TRPA1 Mediates Formalin-Induced Pain. *Proceedings of the National Academy of Sciences* **2007**, *104*, 13525–13530, doi:10.1073/pnas.0705924104.
35. Holzer, P. The Pharmacological Challenge to Tame the Transient Receptor Potential Vanilloid-1 (TRPV1) Nocisensor. *Br J Pharmacol* **2008**, *155*, 1145–1162, doi:10.1038/bjp.2008.351.
36. Olsson, M.H.M.; Søndergaard, C.R.; Rostkowski, M.; Jensen, J.H. PROPKA3: Consistent Treatment of Internal and Surface Residues in Empirical p K a Predictions. *J Chem Theory Comput* **2011**, *7*, 525–537, doi:10.1021/ct100578z.
37. Guedes, I.A.; Barreto, A.M.S.; Marinho, D.; Krempser, E.; Kuenemann, M.A.; Sperandio, O.; Dardenne, L.E.; Miteva, M.A. New Machine Learning and Physics-Based Scoring Functions for Drug Discovery. *Sci Rep* **2021**, *11*, 3198, doi:10.1038/s41598-021-82410-1.
38. Guedes, I.A.; Pereira da Silva, M.M.; Galheigo, M.; Krempser, E.; de Magalhães, C.S.; Correa Barbosa, H.J.; Dardenne, L.E. DockThor-VS: A Free Platform for Receptor-Ligand Virtual Screening. *J Mol Biol* **2024**, *436*, 168548, doi:10.1016/j.jmb.2024.168548.
39. Sakurada, T. Involvement of Spinal NMDA Receptors in Capsaicin-Induced Nociception. *Pharmacol Biochem Behav* **1998**, *59*, 339–345, doi:10.1016/S0091-3057(97)00423-1.
40. Matheus, M.E.; Berrondo, L.F.; Vieitas, E.C.; Menezes, F.S.; Fernandes, P.D. Evaluation of the Antinociceptive Properties from Brillantaisia Palisotii Lindau Stems Extracts. *J Ethnopharmacol* **2005**, *102*, 377–381, doi:10.1016/j.jep.2005.06.033.
41. Sahley, T.L.; Berntson, G.G. Antinociceptive Effects of Central and Systemic Administrations of Nicotine in the Rat. *Psychopharmacology (Berl)* **1979**, *65*, 279–283, doi:10.1007/BF00492216.

 doi:10.20944/preprints202504.2053.v1